Published in final edited form as:
Nat Neurosci. 2019 November ; 22(11): 1844–1856. doi:10.1038/s41593-019-0495-z.

Associative conditioning remaps odor representations and modifies inhibition in a higher olfactory brain area

Thomas Frank[1,*], **Nila R Mönig**[1,2], **Chie Satou**[1], **Shin-ichi Higashijima**[3], **Rainer W Friedrich**[1,2,*]

[1]Friedrich Miescher Institute for Biomedical Research, Basel, Switzerland [2]University of Basel, Basel, Switzerland [3]National Institutes of Natural Sciences, Exploratory Research Center on Life and Living Systems, National Institute for Basic Biology, Okazaki, Japan

Abstract

Intelligent behavior involves associations between high-dimensional sensory representations and behaviorally relevant qualities such as valence. Learning of associations involves plasticity of excitatory connectivity but it remains poorly understood how information flow is reorganized in networks and how inhibition contributes to this process. We trained adult zebrafish in an appetitive odor discrimination task and analyzed odor representations in a specific compartment of telencephalic area Dp, the homolog of olfactory cortex. Associative conditioning enhanced responses with a preference for the positively conditioned odor (CS^+). Moreover, conditioning systematically remapped odor representations along an axis in coding space that represented attractiveness (valence). Inter-individual variations in this mapping predicted variations in behavioral odor preference. Photoinhibition of interneurons resulted in specific modifications of odor representations that mirrored effects of conditioning and reduced experience-dependent, inter-individual variations in odor-valence mapping. These results reveal an individualized odor-to-valence map that is shaped by inhibition and reorganized during learning.

*Correspondence: Dr. Rainer Friedrich, Rainer.Friedrich@fmi.ch, Phone: +41 61 697 9614; Dr. Thomas Frank, Thomas.Frank@fmi.ch, Phone: +41 61 697 8597.

Data availability

The data that support the findings of this study are available from the corresponding authors upon reasonable request.

Code availability

All code used in this study is available from the corresponding authors upon reasonable request.

Author Contributions

T.F. conceived the project, designed experiments, generated transgenic fish lines, performed all experiments except for behavioral conditioning, analyzed data, interpreted data, and wrote the manuscript. N.R.M performed and analyzed behavioral conditioning experiments and commented on the manuscript. C. S. performed and analyzed behavioral conditioning experiments and commented on the manuscript. S. H. generated transgenic fish lines and commented on the manuscript. R.W.F. conceived the project, designed experiments, interpreted data, and wrote the manuscript.

Competing Financial Interests Statement

The authors declare no competing interests.

ORCID: Rainer Friedrich: 0000-0001-9107-0482
ORCID: Thomas Frank: 0000-0002-5113-176X

Europe PMC Funders Author Manuscripts

Introduction

Higher brain functions depend on the interpretation of sensory information based on experience. This process involves associations between high-dimensional sensory inputs and low-dimensional, fundamental qualities such as valence[1,2]. Associative computations are thought to be a main function of piriform cortex (PC), a paleocortical area with prominent recurrent connectivity that lacks an obvious fine-scale topography[3–8]. PC is one of multiple interconnected brain areas that receive sensory input from mitral cells of the olfactory bulb (OB)[3], where odors are represented by normalized and decorrelated activity patterns[9–13]. PC is thought to establish synthetic olfactory object representations by autoassociative memory mechanisms based on activity-dependent modifications of recurrent connectivity[2,3,14]. Consistent with such models, learning modified odor responses, pattern separation and pattern completion in PC[15–17]. Moreover, opto- or pharmacogenetic manipulations modified associative memories[18–20] and ablation of posterior PC impaired temporally remote olfactory fear memory[21]. Nevertheless, mechanisms of memory formation in PC are still poorly understood and it remains unclear how odor representations are associated with behaviorally relevant qualities such as valence.

Models of memory networks often assume that learning is mediated by specific modifications of excitatory synaptic connections[2] while inhibition is primarily homeostatic. In theory, however, specific inhibitory interactions could further enhance memory functions. For example, co-tuning of excitation and inhibition can stabilize memory states[22], and inhibitory response components may shape tuning curves and population activity. However, the hypothesis that specific changes in inhibition contribute to the experience-dependent reorganization of information processing has been difficult to address experimentally. In PC, results obtained in naïve animals suggest that inhibition is broadly tuned[23] but it remains to be examined how inhibitory subnetworks are modified during learning.

We examined the plasticity of odor representations in the zebrafish homolog of olfactory cortex, the posterior zone of the dorsal telencephalon (Dp)[24]. Projections from the OB to Dp lack a topographic organization[25] and odors evoke distributed activity patterns across Dp neurons[26,27]. Repeated passive odor exposure results in an N-methyl-D-aspartate (NMDA) receptor-dependent adaptation and reorganization of odor-evoked activity patterns, consistent with activity-dependent plasticity of odor processing in Dp[28]. Here we trained adult zebrafish in an odor discrimination task and measured activity patterns in a dorsal-posterior subregion of Dp (dpDp) that had not been characterized in detail in previous studies[26–29]. Associative conditioning had pronounced effects that were partially reversed by photoinhibition of GABAergic interneurons. These results indicate that associative conditioning remaps odor space onto a low-dimensional, behaviorally relevant representation of valence by a process that modifies inhibition.

Results

Odor representations in dorsal posterior Dp (dpDp)

We measured activity patterns in a dorsal posterior subregion of Dp (dpDp) by two-photon Ca^{2+} imaging in an *ex-vivo* preparation of the brain and nose after bolus loading of Oregon

Green 488 BAPTA-1-AM (Online Methods; Fig. 1a,b)[27]. We quantified olfactory responses to four amino acids (Ala, Trp, His, Ser; 10^{-4} M), which are natural odorants (Fig. 1b-e). Population activity was dense (53 ± 4 % of neurons active per stimulus; mean ± s.d. across odors, n = 1790 neurons, N = 13 animals), but was typically dominated by a few strongly responsive neurons (population sparseness: 0.38 ± 0.09; mean ± s.d. across animals). The mean lifetime sparseness, a measure for tuning sharpness, was low (0.07 ± 0.08; mean ± s.d. across neurons). Hence, neurons in dpDp were more broadly tuned than neurons in other subregions of Dp[27] or in the OB[30].

To analyze population activity, we averaged Ca^{2+} signals during a two-second time window after response onset and described activity patterns by vectors across neurons. Distances between patterns were quantified by the cosine distance, $1 - \cos(\alpha)$, where α is the angle between vectors. This measure is closely related to the Pearson correlation coefficient but independent of response intensity, which allowed us to separately analyze effects on the structure and on the intensity of population activity patterns. Pairwise distances between odor-evoked activity patterns were modest (range: 0.05 to 0.09) and the corresponding Pearson correlation coefficients were relatively high (range: 0.76 to 0.86), implying that patterns overlapped substantially (Fig. 1f). Pattern discriminability was quantified using a classifier that assigns individual trials to odors by matching activity vectors to templates constructed from other trials based on the lowest cosine distance. Using this cross-validation procedure, classification success was significantly above chance (25%; $p < 10^{-15}$; Fig. 1g) but below 100% ($p = 4x10^{-10}$) and below the success rate of odor classification based on activity patterns from the OB[30] or from other subregions of Dp. Similar results were obtained when Pearson correlation or Euclidean distance were used as a distance metric (Supplementary Fig. 1) or when linear discriminant analysis was used for classification (not shown). Hence, odors evoked dense population activity in dpDp that was informative about odor identity but not optimized for precise odor identification by simple classifiers.

Associative olfactory conditioning

We next examined how odor representations in dpDp are modified by experience. We first analyzed innate behavioral responses to four amino acids (Ala, Trp, His, Ser) by infusing them into tanks containing individual, naïve adult zebrafish (Supplementary Fig. 2a, b). Ala evoked a transient increase in swimming speed (Fig. 2a) that was reminiscent of appetitive behavior[31] (Ala vs tank water, p = 0.0006), consistent with a previous report that Ala is innately attractive[32]. Trp, His, or Ser, in contrast, had no obvious effects compared to control (tank water) trials, indicating that these amino acid odors were neutral (odor vs tank water, p > 0.5 in all cases).

We then trained adult zebrafish in an associative odor discrimination task (Fig. 2b-d)[33]. Briefly, individual fish were exposed once every 20 min to one of two conditioned odors (CS^+, CS^-). The positively conditioned stimulus (CS^+) predicted the delivery of a food reward (unconditioned stimulus, US) into a feeding ring 30 s after stimulus onset while the CS^- remained unrewarded. Fish received nine CS^+ trials and nine CS^- trials per day and were trained for three or four days. One set of fish (ALA) was trained on Ala as CS^+ and Trp as CS^-, a second set of fish (TRP) was trained on Trp as CS^+ and Ala as CS^-, and a third set of

fish (HIS) was trained on His as CS^+ and Ala as CS^-. Behavioral responses were measured during the 30 s after odor onset by quantifying multiple components of appetitive behavior including swimming speed, the height in the water column, and the presence in the reward area (Supplementary Fig. 2d-f). Behavioral measures were then normalized and combined to obtain a composite behavioral score for appetitive behavior (ζ, Online Methods)[33]. Statistically significant differences between behavioral responses to the CS^+ and CS^- emerged already on the first day of training and approached saturation on the third day (Fig. 2d; day 1, $p = 0.003$; day 2, $p = 1x10^{-5}$; day 3, $p = 3x10^{-9}$, N = 43 animals), consistent with previous observations[33]. Five out of six individual behavioral components exhibited significant differences on the second and third day, showing that results were not dominated by a single behavioral readout (Supplementary Fig. 2f). No difference was observed between the three training cohorts ($p = 0.50$, ANOVA; Supplementary Fig. 2c). Hence, fish rapidly learned to establish associations between specific odors and an appetitive behavioral program.

In an additional group of fish (UNC) we temporally uncoupled the CS (Ala or Trp) and US by delivering food 15 min after odor presentation pseudo-randomly in 50% of all trials. Hence, fish received the same number of odor stimuli and the same number of food applications as in associative conditioning, but odor stimulation was not immediately followed by food and did not predict reward (Fig. 2e). In this control experiment, fish did not systematically develop differential appetitive responses to Ala and Trp ($p \geq 0.15$ on all days; Fig. 2f).

Experience modifies odor responses in dpDp

To analyze effects of learning on olfactory processing we compared odor responses in dpDp between fish of five experimental groups: ALA (N = 12 animals), TRP (N = 16), HIS (N = 15), UNC (N = 12) and naïve fish (NAV; N = 13). The majority of fish (12 ALA, 13 TRP, 8 UNC and 9 NAV fish) originated from the same crossing (Online Methods). An initial analysis of basic response properties in this subpopulation revealed that responses averaged over all odors were significantly higher than in NAV fish after training in an associative paradigm (ALA, TRP; $p < 10^{-13}$) but not after uncoupled odor exposure (UNC; $p = 0.30$), (Fig. 3a). This increase in the mean odor response of conditioned fish (ALA, TRP) was due to an increase in the response amplitude of individual neurons rather than the fraction of odor-responsive neurons (not shown). Moreover, changes in response amplitude relative to NAV fish were larger for the CS^+ than for the CS^-: in ALA fish, responses to Ala were increased more than responses to Trp ($p = 1x10^{-5}$), whereas in TRP fish, responses were increased to Trp but not to Ala ($p = 0.005$; Supplementary Fig. 3a). As a consequence, the amplitude ratio (Ala/Trp) was significantly shifted in the direction of the CS^+ when compared to NAV (ALA: $p = 0.0006$, TRP: $p = 6x10^{-5}$; Fig. 3b). The Ala/Trp response ratio in UNC fish, in contrast, was not significantly different from NAV ($p = 0.09$). Conditioning also changed the signal-to-background ratio of odor responses, which is defined for each neuron as the response amplitude normalized to the signal fluctuations during spontaneous and odor-evoked activity[34] (Supplementary Fig. 3b, c).

The remaining subpopulation of fish originated from two additional crossings and included HIS fish (4 NAV fish, 3 TRP fish, 15 HIS fish, and 4 UNC fish). The absolute amplitude of odor responses in this subpopulation was slightly but significantly different from the first subpopulation (ca. 10% reduction in NAV fish, $p = 0.003$; Supplementary Fig. 3d), which may reflect differences in genetic background and precluded direct comparisons of response amplitudes between HIS fish and other groups. However, in HIS fish, responses to the CS^+ (His) were significantly increased when compared to NAV fish from the same crossings (155% ± 3% (mean ± s.e.m.) of NAV, n = 528; HIS, n = 2040; $p < 10^{-16}$; Wilcoxon-Mann-Whitney test, two-sided) consistent with findings in the first subpopulation. To allow for comparisons across crossings, further analyses were based on response ratios. The ratio of CS response amplitudes (Ala/His; $p = 4x10^{-10}$; Fig. 3b) and the corresponding signal-to-background ratio (Supplementary Fig. 3c) were shifted towards the CS^+ when compared to NAV fish. Hence, responses to the CS^+ and CS^- were consistently shifted in the direction of the CS^+ in all conditioned groups.

To examine the relationship between neuronal response amplitudes in dpDp and behavioral responses to odors we quantified odor preference at the end of training by the difference d between ζ scores for Ala versus Trp or His ($d = \zeta_{Ala} - \zeta_{Trp\ or\ His}$; d = 0: no preference; d > 0: preference for Ala; d < 0: preference for Trp or His). The behavioral preference for the CS^+ was correlated to the relative amplitude of the CS^+ response after associative conditioning (ALA, TRP, HIS): stronger neural responses to the CS^+ predicted stronger behavioral preference for the CS^+ across individuals ($r = 0.37$, $p = 0.02$, N = 43 animals; Fig. 3c). In the same fish, the amplitude ratio of responses to odors that were not used in conditioning (Ser versus His or Trp) was not related to behavioral preference ($r = 0.00$, $p = 1$; Fig. 3d). Moreover, the Ala/Trp response ratio did not predict behavioral preference in UNC fish ($r = –0.22$, $p = 0.49$; Supplementary Fig. 3e). The relative enhancement of odor responses to the CS^+ therefore partially predicted behavioral preference after associative conditioning.

Further analyses showed that the mean lifetime sparseness of odor responses in ALA, TRP, HIS, and UNC fish was significantly higher than in NAV fish ($p < 10^{-15}$ for all comparisons; Fig. 3e). Consistent with this observation, the slope of tuning curves constructed by rank-ordering of odor responses in individual neurons was significantly increased (Fig. 3f). Neurons in dpDp therefore became more sharply tuned after associative conditioning and uncoupled odor exposure.

Effects of experience on neuronal population activity

Models of olfactory cortex suggest that information storage involves the strengthening of recurrent excitatory connections among specific neurons[14], which may increase the correlation of spontaneous and odor-evoked activity among neuronal subsets. To test this hypothesis, we quantified pairwise correlations between activity traces of simultaneously recorded neurons in the absence of stimuli (spontaneous correlation). On average, spontaneous correlations were positive in NAV fish and significantly increased after associative conditioning or uncoupled odor exposure ($p < 10^{-5}$ for all groups; Fig. 4a). These observations cannot be explained by chance effects because shuffling of trials abolished correlations. Similarly, correlations between tuning curves (signal correlations) of dpDp

neurons in the same individuals were positive in NAV fish and further increased by experience ($p < 10^{-15}$ for all comparisons; Fig. 4b). Across individuals, signal correlations were at chance level in NAV fish ($p = 0.89$; Fig. 4b) but became positive after associative conditioning or uncoupled odor exposure ($p < 10^{-6}$ for all groups; Fig. 4b). These effects cannot be explained by a general increase in activity after conditioning (Supplementary Fig. 3f, g). Associative conditioning and uncoupled odor exposure therefore strengthened pairwise neuronal correlations, consistent with models of autoassociative memory[3,14].

To further analyze effects of experience on the structure of population activity patterns we subtracted the mean matrix of cosine distances between activity patterns in NAV fish (Fig. 1f) from the distance matrices of other experimental groups. The resulting difference matrices (Fig. 4c) reflect effects of experience on the similarity of odor representations, independent of effects on response amplitude. We found that ALA training had small and heterogeneous effects on pairwise pattern distances. On average, differences in cosine distances between ALA and NAV fish were indistinguishable from variability across individual NAV fish (Fig. 4d). TRP and HIS training, in contrast, significantly increased the mean distance between odor representations (TRP, $p = 0.02$; HIS, $p = 0.02$; Fig. 4d). This increase was observed for all odor pairs and was particularly pronounced between representations of the CS^+ (Trp or His) and other stimuli (Fig. 4c). UNC fish showed a trend towards increased pattern distances that was, however, not significant when compared to NAV fish ($p = 0.33$; Fig. 4d).

To test for a more specific reorganization of pattern distances we summed absolute distance values in each individual distance matrix, after centering each matrix on the group-specific mean and subtracting the mean centered distance matrix of NAV fish. This measure detects differences in specific pattern distances even in the absence of a change in the mean cosine distance and was also significantly increased in TRP and HIS fish (TRP, $p = 0.0004$; HIS, $p = 0.02$; Fig. 4e), but not in ALA and UNC fish (ALA, $p = 0.97$; UNC, $p = 0.20$), when compared to NAV fish. Hence, associative conditioning had specific effects on the structure of population activity patterns in dpDp that depended on the association between specific odors and reward. This reorganization of the structure of odor representations was not significant when an intrinsically appetitive odor (Ala) was chosen as CS^+ while the CS^- was intrinsically neutral (Trp or His) but was pronounced when the CS^+ was intrinsically neutral (Trp or His) while the CS^- was intrinsically appetitive (Ala). Hence, the amount of reorganization of odor representations may be related to changes in odor-value associations.

The success of odor identification by template matching of odor-evoked activity patterns was not significantly different between any of the experimental groups (see below). Hence, experience did not significantly facilitate or impair odor identification by a simple classifier, supporting the notion that precise odor identification is unlikely to be a primary function of dpDp.

Mapping odor space onto a representation of valence

Associative conditioning and uncoupled odor exposure affected not only responses to conditioned odors but also modified responses to other odors in an odor- and task dependent fashion, raising the possibility that experience-dependent modifications of odor

representations generalize according to a global logic. We thus asked whether the organization of odor representations in dpDp could be mapped onto a low-dimensional structure that captures variations across individuals and experimental groups. In each fish, we described the organization of odor representations by the six pairwise cosine distances between the four odor-evoked activity patterns (Ala, Trp, His, Ser). The resulting six-element vector therefore characterized the organization of the olfactory coding space and is referred to as the "coding structure" (Fig. 5a). Coding structures of individual fish from all groups (NAV, ALA, TRP, HIS, UNC) were pooled and then analyzed by principal component analysis (PCA).

The first two principal components (PC 1 and PC 2) represented 62% and 15% of the variance, respectively (Fig. 5b). In the space defined by these PCs, coding structures of ALA fish were close to those of NAV fish but partially separated from those of TRP and HIS fish. Coding structures of UNC fish were similar to those of NAV fish, with few exceptions. To further simplify this analysis, we focused on PC 1 which included high loadings (weights) on a subset of distances (Fig. 5c), implying that it did not represent the distance between a single odor pair or the global distance between all odor pairs. After projection onto PC 1, coding structures of TRP and HIS fish were separated significantly from those of NAV fish (TRP, $p = 0.03$; HIS, $p = 0.03$; Fig. 5d) while coding structures of ALA and UNC fish were not significantly different from NAV (ALA, $p = 0.98$; UNC, $p = 0.30$; Fig. 5d). Similar results were obtained when the coding space was not characterized by distances between odors of defined identity (e.g., Ala vs Trp) but by distances between stimuli representing task-relevant categories (e.g. CS^+ vs CS^-; Supplementary Fig. 4a). These results show that effects of different behavioral manipulations can be represented to a large extent by modifications of coding structures along a single, dominant dimension.

We next examined the relationship between the organization of coding space and behavioral odor preference. In UNC fish, which had not learned to associate specific odors with reward, behavioral odor preference ($d = \zeta_{Ala} - \zeta_{Trp}$) was significantly correlated to the PC 1 score ($r = 0.74$, $p = 0.006$; Fig. 5e). Hence, a high PC 1 score predicted a preference for Ala while a low PC 1 score predicted a preference for Trp. In fish that were trained in an associative paradigm (ALA, TRP, HIS), behavioral preference values were distributed over a broader range. Nevertheless, the correlation between the behavioral odor preference d and the PC 1 score remained significant across all experimental groups ($r = 0.52$, $p = 4x10^{-5}$; Fig. 5f; Supplementary Fig. 4). Correlations also remained significant when scores were obtained by projecting coding structures from a subset of the experimental groups onto PC 1 extracted from the other experimental groups (Supplementary Fig. 5). Shuffling of coding structures, however, reduced or abolished this correlation (Supplementary Fig. 4c, d). Hence, the PC 1 score consistently predicted behavioral odor preference independent of the specific associations between odor and reward in different experimental groups. This indicates that PC 1 represents appetitiveness and that experience modified the representation of odors along this dimension. Experience may also modify odor representations along other dimensions but we did not observe a significant correlation between other principal components and behavioral odor preference (Supplementary Fig. 4g). Consistent with the low dimensionality of dpDp representations, the variance represented by PC 1 remained high in a dataset containing responses to eight odors (28-dimensional coding structures; naïve

fish; Supplementary Fig. 4f), but experiments using additional odors are required to assess the precise dimensionality of behaviorally relevant dpDp representations. In summary, dpDp maps odor representations onto an internal variable that is directly related to behavior. We will refer to this internal variable as valence[35].

Experience-dependent modification of inhibition

Memory storage depends not only on modifications of excitatory interactions but also includes inhibitory interactions that may shape neuronal tuning curves and activity patterns. To examine potential functions of inhibition we targeted halorhodopsin-YFP (eNpHR3.0YFP)[36] to GABAergic interneurons (INs) using a transgenic line that contained a Tg(*gad1b:Gal4*) driver and a Tg(*UAS:eNpHR3.0YFP*) responder (Online Methods). In adult fish, eNpHR3.0YFP was detected in scattered somata and fibers throughout Dp (Fig. 6a; Supplementary Fig. 6a). Because the membrane association of eNpHR3.0YFP complicated the detection of somata within the densely labelled neuropil we also examined a Tg(*gad1b:GFP*) line that expressed cytosolic GFP under the control of the same promoter[37]. GFP-positive somata were particularly dense below the anterior nucleus taeniae but scattered GFP-positive somata were found throughout Dp, consistent with previous observations[38]. To hyperpolarize INs in a subset of trials, orange light (594 nm) was directed at Dp through an optical fiber (Fig. 6b) for 6.2 s, starting approximately 500 ms before the onset of odor stimulation. This approach allowed us to compare activity across the same neurons under control conditions and during photoinhibition of INs ("PIN").

PIN significantly increased spontaneous activity and odor responses (Fig. 6c-e; Supplementary Fig. 6b). When compared among fish from the same crossing, the PIN-induced increase of responses was significantly higher after associative conditioning or uncoupled odor exposure than in NAV fish ($p < 10^{-12}$, for all groups; Fig. 6f). These observations show that experience increased inhibitory components of odor responses.

We next examined subtractive and divisive effects of inhibition. Uniform subtractive inhibition decreases all responses by a constant amount, which can sharpen tuning and sparsify activity patterns. This form of inhibition has been observed in PC upon silencing of somatostatin-expressing INs[34]. Uniform divisive inhibition, in contrast, decreases activity by a constant factor and scales activity patterns without modifying their structure or sparseness. To determine whether effects of inhibition are better described by a subtractive or by a divisive model, we fitted a linear function to all responses of individual neurons (Fig. 6g). In NAV fish, the slope of the linear fit was significantly greater than unity ($m = 1.35 \pm 0.33$, mean ± s.d.; $p = 1x10^{-5}$, bootstrap test, one-sided, N = 13 animals) while the y-intercept was close to zero ($Y_0 = 1.05 \pm 0.81$, mean ± s.d.), consistent with primarily divisive inhibition. The relative contribution of subtractive and divisive components was quantified by the relative contributions of the offset and the slope of the fit, respectively, to the mean PIN-induced response enhancement. This analysis confirmed that the divisive component of inhibition dominated over the subtractive component in all experimental groups (Fig. 6h). Associative conditioning and uncoupled odor exposure therefore enhanced inhibition without major changes in the relative contribution of subtractive and divisive components.

Further analyses showed that PIN reduced the signal-to-background ratio (Supplementary Fig. 6d) and significantly reduced the mean lifetime sparseness of odor responses (NAV, $p = 2x10^{-12}$; ALA, $p = 8x10^{-67}$; TRP, $p = 2x10^{-82}$; HIS, $p = 4x10^{-41}$; UNC, $p = 0.004$; Fig. 7a). In fish that underwent associative conditioning (ALA, TRP, HIS), but not in UNC fish, this reduction was significantly larger than in NAV fish (Fig. 7a). Changes in inhibitory interactions are therefore likely to contribute to the sharpening of odor responses during associative conditioning. Across all groups that underwent associative conditioning (ALA, TRP, HIS), the relative amplitudes of responses to the CS^+ and CS^- during PIN remained correlated to behavioral odor preference in individual fish ($r = 0.35$; $p = 0.02$; Fig. 7b). No systematic relationship was observed between the amplitude ratio of responses to non-conditioned odors (Ser versus His or Trp) during PIN and behavioral odor preference ($r = -0.09$, $p = 0.58$; Fig. 7c). The CS^+/CS^- response ratio during PIN therefore still predicted behavioral odor preference after conditioning, as observed under control conditions. Classification of odor-evoked activity patterns by template matching was not significantly different during PIN in any of the experimental groups (Fig. 7d).

Inhibition may contribute to systematic modifications of odor-evoked activity patterns after experience. If so, inhibitory components of odor responses should have two properties. First, inhibition in individual neurons should not be uniform across odors but exhibit non-uniform components that shape odor tuning. Second, effects of experience on the tuning of inhibition should be coordinated across different neurons to shape population activity patterns in a systematic fashion.

Consistent with non-uniform inhibition in individual neurons, linear models of inhibition did not fully explain the effects of PIN on odor responses, as indicated by the substantial scatter around linear fits (cf. Fig. 6g). More detailed analyses of individual neurons showed that effects of PIN on odor responses were nearly uniform in some neurons but highly odor-dependent in others (Fig. 7e). To further characterize non-uniform inhibition, we measured the relative PIN-induced response change for each neuron-odor pair by a change index that varies between –1 and 1 (Online Methods). A low variation of the change index across odors implies that effects of PIN are largely uniform (divisive), while a high variation implies non-uniform inhibition. We therefore define the standard deviation (s.d.) of the change index as a "non-uniformity index" for each neuron. As a control, we used the same procedure to compare successive trials with the same odors under the same conditions (control-control or PIN-PIN). The non-uniformity index was significantly higher than the control indices in all experimental groups ($p < 10^{-19}$, for all comparisons; Fig. 7f), confirming that inhibition had significant non-uniform effects on individual neurons.

Remapping of odor-valence relationships involves inhibition

To explore whether non-uniform inhibition is coordinated across the population we examined effects of PIN on cosine distances between odor-evoked activity patterns. If inhibitory components of odor representations are uncoordinated, effects of PIN are expected to be unspecific and global. However, we found that effects of PIN systematically depended on the odor and task. PIN significantly decreased cosine distances between odor-evoked activity patterns in all groups except NAV (Fig. 8a, b). As a consequence, differences

in pattern distances between experimental groups disappeared (Supplementary Fig. 6e, f). Furthermore, the pattern of PIN-induced distance changes was similar in structure, but opposite in sign, to the pattern of distance changes induced by associative conditioning or uncoupled odor exposure in each experimental group. Consistent with this observation, PIN-induced distance changes were negatively correlated to experience-related distance changes across all fish and odor pairs (ALA, r = –0.77; TRP, r = –0.80; HIS, r = –0.81; UNC, r = –0.50; Fig. 8c). These results show that inhibitory response components systematically depended on associations between odors and reward, implying that effects of inhibition were coordinated across the population of neurons in dpDp.

The observation that effects of PIN on odor representations in dpDp were mirror-symmetric to effects of experience (Fig. 8b, c) indicates that changes in inhibitory response components contributed significantly to the reorganization of odor representations during associative conditioning. To corroborate this conclusion, we projected coding structures onto the first two principal components and found that PIN reduced distances between coding structures from different experimental groups (Fig. 8d, Supplementary Fig. 6g). This observation cannot be explained by a change in response amplitudes because coding structures were defined by cosine distances. Moreover, in other distance metrics, a non-specific increase in response amplitude would be expected to increase, rather than decrease, differences between activity patterns. Hence, PIN had specific effects on coding space that were opposite to those of experience, consistent with the hypothesis that experience-dependent reorganizations of coding space included coordinated plasticity of inhibitory response components.

This conclusion was further supported by the observation that PIN-induced changes in PC 1 scores were negatively correlated to the PC 1 score under control conditions: a large initial PC 1 score predicted a large PIN-induced change of opposite sign (Fig. 8e; over all fish, r = –0.74, $p = 4x10^{-13}$, N = 68 animals; see also Supplementary Fig. 6h). Hence, PIN systematically reduced inter-individual variations in odor-valence mappings across all experimental groups. Nevertheless, PIN did not fully abolish differences in PC 1 scores between experimental groups. Moreover, the PC 1 scores during PIN, although reduced, still showed a residual positive correlation to behavioral odor preference (Supplementary Fig. 6j, k). These observations indicate that the observed modifications of excitatory response components (cf. Fig. 3a) also contribute to inter-individual variations in odor-value maps. Our results therefore indicate that experience results in coordinated modifications of excitatory and inhibitory interactions that both contribute to the remapping of odor space onto an axis of valence in dpDp.

Discussion

Our results revealed multiple effects of experience on odor-evoked activity in dpDp that collectively had two major consequences. First, associative conditioning enhanced the representation of the CS^+ relative to the representation of the CS^-. Second, manipulations of odor-reward associations remapped representations of odors along a behaviorally relevant axis of valence in an experience-dependent fashion. Remapping of odor representations involved a global increase in inhibition as well as specific effects on inhibitory components of neuronal tuning curves, as revealed by PIN. Hence, modifications of inhibitory response

components play an instructive role in the experience-dependent reorganization of odor-valence associations in dpDp.

Experience-dependent remapping of odor representations

Unlike odor-evoked activity in other subregions of Dp[26,27] and in subregions of parts of PC[4,5,7,8,39], odor responses in dpDp were dense and not very odor-selective. Activity in dpDp represented a combination of sensory and task-related information, which is generally consistent with neuronal activity in posterior PC[40–42]; the phylogenetic relationships, however, between subregions of Dp and mammalian olfactory cortex remain to be clarified. To manipulate odor-value associations we conditioned a familiar feeding behavior on olfactory cues[33]. Although activity was measured in an *ex-vivo* preparation after conditioning, multiple features of neuronal activity were highly correlated to inter-individual variations in odor preference. Activity patterns therefore reflected behaviorally relevant variations in neuronal circuit function.

Associative conditioning and uncoupled odor exposure enhanced correlations of spontaneous activity and odor responses between individual neurons, consistent with predictions of autoassociative memory models. However, most memory models consider a regime of high dimensionality and high memory capacity[2]. The high pattern and signal correlations in dpDp, in contrast, indicate that activity in dpDp is low-dimensional and not optimized for high storage capacity, consistent with the hypothesis that dpDp maps odor responses onto a low-dimensional output.

One effect of associative conditioning was a general enhancement of odor responses that was more pronounced for the CS^+ than for the CS^-. Enhanced representations of rewarded stimuli have also been observed in other brain areas including auditory and visual cortex[43–46]. In these brain areas, conditioning usually increases the discriminability of stimulus representations, suggesting that plasticity supports perceptual learning. In dpDp, in contrast, experience did not affect pattern discriminability, suggesting that enhanced responses primarily increase the impact of rewarded stimuli onto appetitive behavior.

A second main effect of associative conditioning was a systematic reorganization of olfactory coding space in dpDp along a dimension closely related to valence. Inter-individual variations in the organization of olfactory coding space predicted variations in behavioral odor preference across experimental groups and even among individuals within the same group. Hence, dpDp maps odor space onto a low-dimensional representation of valence that is modified by experience and likely to have a direct influence on appetitive behavior. These results are consistent with the notion that the dimensionality of perceptual space in olfaction is low although the dimensionality of chemical stimulus space may be high[47].

The finding that the organization of odor representations predicted appetitive behavior across individuals implies that associative learning modified coding space while the valence axis remained consistent. This indicates that the quality of information transmitted by individual neurons remains stable when odor-value associations change, which is important when neurons have defined effects on behavior. Associative learning by a reorganization of coding

Europe PMC Funders Author Manuscripts

Europe PMC Funders Author Manuscripts

space is thus a useful strategy in networks that operate close to outputs controlling behavior. In Drosophila, valence is encoded by a dense population code across mushroom body output neurons that project to specific target areas[35,48]. In this system, valence is represented along a fixed axis while the mapping of odors onto this axis can be modified by experience[49], similar to our observations in dpDp. Hence, vertebrates and insects may use similar strategies to associate odors with low-dimensional, internal variables.

Experience-dependent plasticity of inhibition

To manipulate inhibition we expressed eNpHR3.0YFP under the control of the *gad1b* promoter, which targets interneurons broadly. PIN resulted in a pronounced disinhibition in dpDp but incomplete suppression of action potential firing in subsets of interneurons cannot be excluded. Nonetheless, effects of PIN were highly correlated to inter-individual variations in odor-evoked activity and behavior (Fig. 8 and Supplementary Fig. 6), implying that effects of PIN were reliable and effective across individuals.

In PC, photoinhibition of somatostatin-expressing interneurons revealed a form of global subtractive inhibition[34] whereas our more broadly targeted approach revealed primarily divisive inhibition in dpDp. Divisive inhibition can efficiently normalize activity in autoassociative networks, which is important to counterbalance recurrent amplification[22]. Consistent with such a function, PIN unmasked an enhancement of divisive inhibition after associative conditioning that partially balanced the increase in excitatory odor responses.

Inhibition also had non-uniform effects on tuning curves that were systematically modified by associative conditioning, resulting in coordinated changes of inhibitory response components across the population. The underlying synaptic modifications may involve multiple cell types and connections. In principle, specific modifications of inhibition may be indirect consequences of plasticity at synapses between excitatory neurons. Alternatively, modifications of inhibition may involve plasticity of synapses from excitatory neurons to INs, from INs to excitatory neurons, or both. This hypothesis is consistent with the complex non-uniform effects of PIN and their specific contributions to odor-valence mapping. Moreover, this scenario is consistent with the observation that inhibitory inputs to neurons in posterior Dp exhibit non-random tuning[29], and with learning-dependent changes in the response selectivity of INs in other brain areas[50].

Coordinated plasticity of inhibitory response components contributed significantly to experience-dependent plasticity of odor representations in dpDp. PIN reduced inter-individual variations in PC scores, even among NAV fish, resulting in the convergence of coding structures towards a common “baseline state”. Moreover, effects of PIN mirrored effects of experience on pairwise distances between activity patterns across all odors and fish. Hence, a substantial fraction of task-dependent changes and other inter-individual variations in odor-value maps can be explained by variations in patterned inhibition. However, PIN did not completely abolish remapping of odor representations, suggesting that plasticity of interactions between excitatory neurons also contributed to the reorganization of odor responses. These results suggest that inhibitory network plasticity enhances excitatory plasticity particularly during specific memory operations.

Online Methods

Animals and transgenic lines

All experiments were performed using adult zebrafish (*Danio rerio*) of both sexes, aged 7 ± 4 months (mean ± s.d.). Fish were raised and kept under standard laboratory conditions (26 – 27 °C; 13 h/11 h light/dark cycle). With few exceptions (below), experiments were performed in a double-transgenic line that expressed the light-sensitive chloride pump halorhodopsin (eNpHR3.0[36]) fused to yellow fluorescent protein (YFP) under the control of the glutamate decarboxylase 1b promoter Tg(*gad1b:Gal4, UAS:eNpHR3.0YFP*). These fish ('gad1b-NpHR') originated from three different crossings (each crossing: ≤5females and ≤ 5 males). Most fish (9 NAV, 12 ALA, 13 TRP, and 8 UNC) originated from the first crossing. The remaining fish (4 NAV, 3 TRP, 15 HIS, and 4 UNC) originated from two additional crossings of other individuals. All fish used in the study were assigned randomly to the different training groups. For activity measurements and analysis of innate behavioral odor preference, naïve fish were chosen randomly from large populations (> 40) of gad1b-NpHR fish. Exceptions (non gad1b-NpHR fish): Fig. 6a (Tg(*gad1b:GFP*)[37], N = 3 animals); Supplementary Fig. 4f (mixed population of naïve adult zebrafish, N = 15 animals); Supplementary Fig. 6c (Tg(*UAS:eNpHR3.0YFP*), N = 2 animals). Experiments were approved by the Veterinary Department of the Canton Basel-Stadt (Switzerland).

To target optogenetic probes to GABAergic interneurons in Dp we used the promoter of the *gad1b* gene (formerly *GAD67*), which encodes one of the two major isoforms of glutamate decarboxylase in zebrafish[51]. To enhance the visualization of somata we also analyzed Tg(*gad1b:GFP*) fish[37]. Throughout Dp, the number and distribution of somata expressing eNpHR3.0YFP in Tg(*gad1b:Gal4, UAS:eNpHR3.0YFP*) fish and GFP in Tg(*gad1b:GFP*) fish were comparable to each other and consistent with the reported expression of *gad1b* mRNA in adult zebrafish[38]. A high density of positive somata was found posterior to the prominent medio-lateral furrow that runs along the anterior border of the nucleus taeniae. In addition, scattered somata and dense fibers were observed throughout the volume of Dp (Fig. 6a). The number of positive somata was substantially higher than in other transgenic lines that target distinct subsets of interneurons in Dp (T.F. and R.W.F., unpublished observations). This indicates that the *gad1b* promoter targeted multiple subtypes of interneurons that account for the majority of, possibly all, interneurons in Dp.

The UAS:eNpHR3.0YFP expression construct was generated using the Tol2Kit[52], involving a multisite recombination reaction (Invitrogen Multisite Gateway manual Version D, 2007) between p5E–UAS (5xUAS and E1b minimal promoter[53]), pME–eNpHR3.0YFP (third-generation halorhodopsin fused to YFP[36]), and p3E–polyA as entry vectors, and pDestTol2CG2 as destination vector[52]. A stable transgenic founder line was generated using standard procedures[54].

Fish expressing Gal4 under the *gad1b* promoter Tg(*gad1b:Gal4*) were generated using the BAC (bacterial artificial chromosome) homologous recombination technique with the Tol2-mediated method[55]. The BAC clone zC24M22 was used, into which a hsp70-Gal4 (Gal4FF)[56] DNA construct was introduced[55].

Experimental preparation, dye loading and odor application

Ca^{2+} imaging was performed in an *ex-vivo* preparation of the entire zebrafish brain and nose[27]. Briefly, adult zebrafish were cold-anesthetized, decapitated, and the forebrain was exposed ventrally after removing the eyes, jaws and palate. The preparation was placed in a custom-made flow-chamber, continuously superfused with teleost artificial cerebrospinal fluid (ACSF) and slowly warmed up to room temperature. ACSF contained (in mM): 124 NaCl, 2 KCl, 1.25 KH_2PO_4, 1.6 $MgSO_4$, 22 D-(+)-Glucose, 2 $CaCl_2$, 24 $NaHCO_3$, pH 7.2[57].

Activity was measured in a dorsal aspect of Dp, posterior to the anterior commissure and to the furrow at the anterior border of the nucleus taeniae (Fig. 1a). This subregion (dpDp) comprises approximately 10% of the volume of Dp. Bolus loading of Oregon Green 488 BAPTA-1-AM (OGB-1; ThermoFisher Scientific) was performed as described[27], with minor modifications. 50 µg of OGB-1-AM was dissolved in 30 µl of DMSO/Pluronic F-127 (80/20; ThermoFisher Scientific) and stored in 4 µl aliquots at −20°C. Prior to each experiment, an aliquot was diluted 1:5 in ACSF and loaded into a glass pipette with a tip diameter of approximately 5 µm. Pressure injections were targeted to the lateral telencephalon, posterior to the prominent furrow and blood vessel and slightly dorsal to Dp. One or two injections were made ~300 - 350 µm dorsal from the ventralmost aspect of Dp. Progress of dye uptake was monitored by snapshots of multiphoton images and pressure was adjusted to minimize swelling of the tissue. Odor-evoked activity was subsequently measured approximately 100 µm ventral to the injection sites (200 – 250 µm from the ventralmost aspect of Dp). This region contains a scattered band of large neuronal somata that is referred to as dpDp (Fig. 1). Nomenclature of brain areas and drawings showing the location of dpDp (Fig. 1a; Supplementary Fig. 6a) are based on the atlas of the adult zebrafish brain[58]. Odor application started > 1 h after dye injection.

Four amino acids (His, Ser, Ala, Trp; Sigma) were prepared as 100x stock solutions in deionized water (Fluka), vortexed, sonicated, stored at −20°C, and diluted to a final concentration of 10^{-4} M in ACSF immediately before the experiment. Odors were applied in blocks of six trials. In each block, three control and three PIN trials were interleaved. Inter-stimulus intervals (ISIs) were 2.25 min ± 15 s (mean ± s.d.). The sequence of odor blocks was varied across animals to avoid systematic biases, but each experiment was started with either one of the neutral odors, followed by either one of the familiar odors, the second neutral odor, and the second familiar odor. Odors were applied to the nasal epithelium for ~3 s through a constant stream of ACSF using a computer-controlled, pneumatically actuated HPLC injection valve (Rheodyne) as described[27]. No odor stimuli were presented prior to the first stimulus in an experiment to minimize potential effects of passive odor exposure on odor responses[28].

Image acquisition and optical stimulation

Multiphoton calcium imaging in Dp was performed using a custom-built multiphoton microscope[59], a 20x objective (NA 1.0, Zeiss) and Scanimage/Ephus software[60,61]. Fluorescence was excited at 928 nm and emission was detected by a gated GaAsP photomuliplier tube (PMT; Hamamatsu) through a bandpass emission filter (535/50nm). In addition, a narrow blocking filter centered on 594 nm was placed in front of the PMT. Laser

intensity was adjusted in each focal plane to minimize photobleaching. In each trial, images with 256 lines were acquired at 128 ms per frame, starting approximately 33 s before odor onset in each trial. After each trial, the field of view was readjusted to compensate for potential drifts using an automated routine that acquired a small z stack of ± 3 μm (step size, 0.5 μm).

For optical stimulation, orange laser light (594 nm) was directed at posterior Dp through an optical fiber (200 μm diameter; ThorLabs) positioned approximately 100 – 200 μm from the brain surface. While light was directed at posterior Dp, we cannot rule out that scattered also had weak effects in adjacent regions. Pulses of light (450 μs) were coupled into the fiber using a digital micromirror device (DMD; Texas Instruments)[59] and synchronized to every second line of image acquisition. Simultaneously, the PMT was switched off. After data acquisition, every second line was removed from images to exclude lines affected by photostimulation. The same procedure was applied to trials without photostimulation, resulting in final images with 128 lines and a fill fraction of approximately 40% under all conditions. The intensity of orange light at the tip of the fiber, averaged over the duty cycle, was 6 – 8 mW. In Tg(*UAS:eNpHR3.0YFP*) fish that did not carry the *gad1b:Gal4* transgene (N = 2), orange laser light had no detectable effect on neuronal activity (Supplementary Fig. 6c).

Regions of interest (ROIs) were drawn manually over all somata in each image plane, using custom-made software (https://github.com/i-namekawa/Pymagor). To calculate the relative change in fluorescence (ΔF/F) in each ROI, the time series of raw fluorescence, averaged over all pixels, was low-pass filtered by a 2 s rolling average and the baseline fluorescence F was defined as the minimum over all time points. Time series of Ca^{2+} signals were aligned to the start of odor-evoked activity to correct for small variations in stimulus onset times across animals. ΔF/F was averaged over a 2 s time window starting at response onset. This resulted in a time window that was centered approximately on the peak of the population response (Fig. 1d). Variation of the temporal alignment procedure or of the analysis time window had minimal effects on the results.

Behavioral experiments

Associative conditioning was performed as described[33]. Briefly, individual gad1b-NpHR fish were acclimated to the behavioral setup without food (1-3 days) and subsequently trained to associate one odor stimulus (CS^+) with a food reward while a second odor stimulus (CS^-) was not rewarded. Nine trials per odor were delivered each day in odor-alternating sequence (inter-trial interval: 20 min). Fish received 27 - 36 trials of each odor (n = 32.3 ± 4.0 trials, mean ± s.d.; N = 43 animals; no dependence of discrimination performance on total trial number (Pearson correlation): r = −0.20, two-tailed *t* test, p = 0.19)). Swimming trajectories were monitored in 3D. Appetitive behavioral response components included: increased swimming speed, elevated position in water column, increased presence in reward zone, increased surface sampling, decreased distance to odor inflow, and decreased rhythmic circular swimming. These behavioral components were quantified during the 30 s after odor onset and prior to reward delivery by automated analyses routines and combined into a compound score of appetitive behavior, ζ[33]. Odor

preference was measured as the mean difference between ζ scores in response to the CS^+ and CS^- over the last nine trials. Alternative metrics for quantification of overall discrimination performance gave very similar results.

Uncoupled odor exposure was performed using a similar schedule except that food was delivered 15 min after odor presentation and assigned pseudo-randomly to 50% of trials, independent of odor identity. Naïve fish were directly taken from the same populations as fish used for associative conditioning or uncoupled odor exposure.

Behavioral training was performed in blocks. Per block, four to twelve individuals were trained in parallel. After termination of training, fish were ranked according to an initial assessment of their discrimination performance, transferred to single tanks in the fish facility and successively selected for measurements of odor-evoked activity patterns 2.1 ± 1.2 (mean ± s.d.) days after last training day. In total, 49 out of 94 trained fish were used for activity measurements. Five out of 49 fish were excluded due to technical problems during behavioral training (evident only after the fish had been imaged), and one fish was excluded upon failed dissection. The remaining 43 fish (12 ALA, 16 TRP, 15 HIS) comprised individuals with a wide range of preference scores (Supplementary Fig. 2c). Twelve out of 14 additional gad1b-NpHR fish that received uncoupled odor exposure were used for activity measurements 0.9 ± 0.7 (mean ± s.d.) days after last odor exposure; two fish were excluded upon failed dissection. Exclusion criteria were established prior to the start of the study.

When behavioral data from fish from different experimental groups were combined for analysis (Figs. 3, 5, 7 and Supplementary Figs. 3-6) the sign of the discrimination score was adjusted to reflect preference for Ala. Image acquisition and primary data analysis of trained fish were performed blind to the odor-reward association of the respective fish for all ALA fish and 13 out of 16 TRP fish. For the remaining fish, the affiliation to the training group could not be concealed from the experimenter.

To analyze innate behavioral responses to odors, individual gad1b-NpHR fish of both sexes (starved for one day; N = 71 animals) were placed in a modified setup (no feeding ring, inflow and outflow tubes). Each fish was acclimated for at least 30 min and tested only once on one odor (and fish facility water as control). In each application, 1 ml of facility water or odor solution (His, Ser, Ala, or Trp; 10^{-3} M in facility water) was applied to one corner of the tank during 20 s after recording baseline swimming activity. We primarily analyzed swimming speed, which has been directly related to appetitive behavior in other tasks[31,62]. However, differential effects of Ala and the remaining odors were also observed for the distance to the odor application site. Behavioral parameters were normalized to the mean value over 50 s prior to stimulus onset and quantified over 40 s after stimulus onset.

Statistical analysis

No statistical methods were used to predetermine sample sizes but our sample sizes are similar to those reported in previous publications[15,44,50]. *N* indicates the number of animals (experiments) and, unless stated otherwise, *n* indicates number of neurons. Unless stated otherwise, sample means are reported ± their standard error (± s.e.m.).

Europe PMC Funders Author Manuscripts

We tested pooled samples for normality using the Jarque-Bera test. We used a repeated measures *t* test for all paired samples with n > 250. For smaller sample sizes or if the null hypothesis of normality was rejected, we used non-parametric tests: non-parametric Kruskal-Wallis test followed by a Dunn-Hollander-Wolfe test for nonparametric multiple comparisons to one control group (reported p-values are adjusted for multiple comparisons) or Wilcoxon signed-rank test for paired samples.

To compare two samples of categorical data (e.g. correctly identified trials in template matching classification analysis) we used a Pearson's chi-squared test for unpaired samples (reported p-values are not adjusted for multiple comparisons), or a McNemar test with Edward's correction for paired samples.

Correlation between two variables was quantified using either Pearson's correlation or the non-parametric Kendall's rank correlation coefficient (related to the non-parametric Theil-Sen estimator for linear regression).

To test whether the regression slope of linear fits was significantly larger than 1 (Fig. 6), we used bootstrapping to estimate the sampling distribution of the regression slope (sampling with replacement, repeated 10'000 times, one-sided test).

In all statistical tests (implemented in Igor Pro 8, Wavemetrics), $p < 0.05$ was considered statistically significant. In graphical displays, standard significance levels are indicated as follows ($p \geq 0.05$: ns; $p < 0.05$: *; $p < 0.01$: **; $p < 0.001$: ***) and are adjusted for multiple comparisons (using Bonferroni-adjusted significance levels when multiple pair-wise tests, e.g. Pearson's chi-squared test were used on the same data). In graphs, grey dotted lines indicate zero and black or orange dotted lines indicate the median of NAV fish.

Further analyses

Defining responses—For the analysis of signal correlation and SBR (see below), only neurons that responded to at least one odor were considered (criterion: mean Ca^{2+} signal during odor response > 2 x s.d. of Ca^{2+} signal during pre-stimulus phase). Modifying this criterion had no major effect on results.

SBR—To quantify discriminability of odor responses (signal) from the background (spontaneous) activity, we calculated the signal-to-background ratio (SBR) for odor responses in individual trials[63] (cf. Supplementary Fig. 3b):

$$SBR = \frac{(\Delta F/F)_{odor} - (\Delta F/F)_{spont.}}{\sqrt{0.5 \times \left(\sigma^2_{odor} + \sigma^2_{spont.}\right)}}$$

$(\Delta F/F)_{odor}$ and σ^2_{odor}: mean and variance of Ca^{2+} signal during odor response (3 s);

$(\Delta F/F)_{spont.}$ and $\sigma^2_{spont.}$: mean and variance of Ca^{2+} signal before odor response (25.6 s). For odor-specific SBR comparisons (Supplementary Fig. 3c) we only considered neurons that responded to both odors. To compare PIN and control trials (Supplementary Fig. 6d), background activity was determined in separate trials. Neuron-odor pair trials with a Ca^{2+}

signal z-score < 2 were excluded from all SBR analyses; lifting this criterion had no effect on odor-specific SBR comparisons.

Sparseness measures: lifetime and population sparseness—Lifetime and population sparseness were calculated using the metric[64]:

$$Sparseness = \frac{1 - \left(\frac{\sum r_n}{N}\right)^2 / \left(\sum \frac{r_n^2}{N}\right)}{1 - \frac{1}{N}}$$

This normalized metric describes the "peakiness" of a distribution and ranges between 0 (all responses equal) and 1 (all responses zero except one). Lifetime sparseness: distribution of response amplitudes across odors in single neurons. Population sparseness: distribution of response amplitudes to a single odor across neurons.

Cosine distance—The cosine distance of two population vectors x and y was defined as:

$$Cosine\ distance = 1 - \cos(\theta) = 1 - \frac{\sum (x_i y_i)}{\sqrt{\sum x_i^2}\sqrt{\sum y_i^2}}$$

Mean cosine distance matrices were calculated by averaging matrices of individual animals. To assess whether the mean cosine distance, across all six pairwise distances, differed from NAV fish (pattern separation; Fig. 4d, Supplementary Fig. 6e), we subtracted the mean cosine distance matrix of NAV fish from the cosine distance matrices in each individual fish (<Δ Cosine dist.>). To assess differences in the structure of cosine distance matrices in each group (pattern reorganization; Fig. 4e, Supplementary Fig. 6f), we (1) centered cosine distance matrices of each fish by subtracting the mean distance of the corresponding experimental group, (2) subtracted the centered mean NAV matrix from the centered matrix of each fish, and (3) subsequently calculated the mean of the absolute values in the difference matrices (<|Δ Cosine dist.|>). Large values therefore indicate changes in specific distances that cannot be accounted for by a change in the mean distance.

Template matching—Odor classification by template matching[65] was performed by choosing the population response vector of one trial as a test vector and comparing it to reference vectors for each odor (similar to leave-one-out cross-validation). Reference vectors were constructed by averaging over all trials except for the test trial. The test trial was then assigned to the odor that was represented by the reference vector with the lowest cosine distance (cf. Fig. 1g). Similar results were obtained when Pearson correlation distance or Euclidean distance were used (Supplementary Fig. 1). To account for differences in the size of the population vectors between fish we randomly selected n = 95 neurons in each classification (minimum population size across all animals: n = 98). This procedure was repeated 400 times in each fish, using sampling without replacement.

Spontaneous correlation—Spontaneous correlations of Ca^{2+} signals between pairs of neurons from the same animal were calculated over the last 20 s of the pre-stimulus phase of 28 trials (560 s total). Time traces were binned to 1 s bins.

Signal correlation—The analysis of signal correlation was restricted to neuron pairs in which both neurons responded to at least one odor. After determining signal correlations for all pairs in one animal, signal correlations were averaged over all pairs involving each neuron, resulting in a mean signal correlation for each neuron. Further averaging was then performed over neurons. Direct averaging of signal correlations over all pairs gave very similar results. Signal correlations across animals were calculated accordingly.

Analysis of coding structures—The organization of odor representations in dpDp was defined in each fish by the six pairwise cosine distances between all four odor-evoked activity patterns (His, Ser, Ala, Trp). Vectors representing these "coding structures" were pooled across all fish (NAV, ALA, TRP, HIS, UNC; N = 68 animals) and optical stimulation conditions (control and PIN). The resulting 6 x 136 matrix (or its transform), representing a total of 136 coding structures, was the input for PCA (Fig. 5, Supplementary Fig. 4). In each of the six coding structure dimensions, the 136 individual values were centered by subtracting their mean. We did not scale each dimension to unit variance to retain information that may be contained in variance differences between dimensions.

Change index and analysis of non-uniform inhibition—Odor-specific effects of inhibition on individual cells were quantified by the change index:

$$Change\ index\ (ChI) = \frac{(\Delta F/F)_{PIN} - (\Delta F/F)_{control}}{(\Delta F/F)_{PIN} + (\Delta F/F)_{control}}$$

Mean strength of inhibition: mean ChI over odors. Non-uniformity of inhibition: standard deviation of ChIs across odors. Only neurons that were modulated by PIN were considered (criterion: p-value < 0.1 for pairwise comparison between control and PIN trials; Wilcoxon signed rank test, two-sided). Note that with this threshold a selective modulation of one out of the four odor responses (i.e. three out of twelve trials) does not suffice to classify a neuron as PIN-modulated. In NAV fish, 87% of responsive neurons were classified as PIN-modulated using this criterion.

Linear regression—To describe effects of inhibition on odor responses we fitted lines to different combinations of parameters derived from control and PIN responses, respectively (Fig. 6g; Fig. 8c, e; Supplementary Fig. 6h). Fitting was performed using a total least squares procedure, which minimizes the orthogonal distance of the regression line from the data points. Thus, this method does not distinguish between dependent and independent variables and accounts for the equality of measurement errors in the two variables. In the remaining linear regression analyses (Fig. 3c, d; Fig. 5e, f; Fig. 7b, c; Supplementary Figs. 3-6) we used a standard least squares procedure.

Europe PMC Funders Author Manuscripts

Supplementary Material

Refer to Web version on PubMed Central for supplementary material.

Acknowledgements

We thank A. Wanner for custom-made scripts for microscope control, E. Arn Bouldoires for excellent technical assistance, and N. Temiz for help during behavioral training. We are grateful to K. Deisseroth (Stanford University, CA, USA) for DNA constructs containing eNpHR3.0YFP and to R. Köster (Technical Unversity Braunschweig, Germany) for DNA constructs containing the 5xUAS cassette. We thank G. Keller, A. Lüthi, C. Meissner-Bernard and P. Rupprecht for critical comments on the manuscript and members of the Friedrich group for helpful discussions. This work was supported by the Novartis Research Foundation, by the Swiss National Science Foundation (SNF; 31003A_135196 and 310030B_1528331), by fellowships from HFSPO (LT000278/2012-L) and EMBO (ALTF 994-2010) to T.F., and by the European Research Council (ERC) under the European Union's Horizon 2020 research and innovation programme (grant agreement No 742576).

References

1. Ganguli S, Sompolinsky H. Compressed Sensing, Sparsity, and Dimensionality in Neuronal Information Processing and Data Analysis. Annu Rev Neurosci. 2012; 35:485–508. [PubMed: 22483042]
2. Poo M, et al. What is memory? The present state of the engram. BMC Biol. 2016; 14:40. [PubMed: 27197636]
3. Haberly LB. Parallel-distributed processing in olfactory cortex: new insights from morphological and physiological analysis of neuronal circuitry. Chem Senses. 2001; 26:551–576. [PubMed: 11418502]
4. Bolding KA, Franks KM. Complementary codes for odor identity and intensity in olfactory cortex. eLife. 2017; 6:e22630. [PubMed: 28379135]
5. Iurilli G, Datta SR. Population Coding in an Innately Relevant Olfactory Area. Neuron. 2017; 93:1180–1197.e7. [PubMed: 28238549]
6. Miyamichi K, et al. Cortical representations of olfactory input by trans-synaptic tracing. Nature. 2011; 472:191–196. [PubMed: 21179085]
7. Roland B, Deneux T, Franks KM, Bathellier B, Fleischmann A. Odor identity coding by distributed ensembles of neurons in the mouse olfactory cortex. eLife. 2017; 6:e26337. [PubMed: 28489003]
8. Stettler DD, Axel R. Representations of Odor in the Piriform Cortex. Neuron. 2009; 63:854–864. [PubMed: 19778513]
9. Banerjee A, et al. An Interglomerular Circuit Gates Glomerular Output and Implements Gain Control in the Mouse Olfactory Bulb. Neuron. 2015; 87:193–207. [PubMed: 26139373]
10. Gschwend O, et al. Neuronal pattern separation in the olfactory bulb improves odor discrimination learning. Nat Neurosci. 2015; 18:1474–1482. [PubMed: 26301325]
11. Kato HK, Gillet SN, Peters AJ, Isaacson JS, Komiyama T. Parvalbumin-Expressing Interneurons Linearly Control Olfactory Bulb Output. Neuron. 2013; 80:1218–1231. [PubMed: 24239124]
12. Niessing J, Friedrich RW. Olfactory pattern classification by discrete neuronal network states. Nature. 2010; 465:47–52. [PubMed: 20393466]
13. Zhu P, Frank T, Friedrich RW. Equalization of odor representations by a network of electrically coupled inhibitory interneurons. Nat Neurosci. 2013; 16:1678–1686. [PubMed: 24077563]
14. Wilson DA, Sullivan RM. Cortical Processing of Odor Objects. Neuron. 2011; 72:506–519. [PubMed: 22099455]
15. Chapuis J, Wilson DA. Bidirectional plasticity of cortical pattern recognition and behavioral sensory acuity. Nat Neurosci. 2012; 15:155–161.
16. Roesch MR, Stalnaker TA, Schoenbaum G. Associative Encoding in Anterior Piriform Cortex versus Orbitofrontal Cortex during Odor Discrimination and Reversal Learning. Cereb Cortex. 2007; 17:643–652. [PubMed: 16699083]

17. Shakhawat AM, et al. Visualizing the engram: learning stabilizes odor representations in the olfactory network. J Neurosci. 2014; 34:15394–15401. [PubMed: 25392506]
18. Choe HK, et al. Oxytocin Mediates Entrainment of Sensory Stimuli to Social Cues of Opposing Valence. Neuron. 2015; 87:152–163. [PubMed: 26139372]
19. Choi GB, et al. Driving Opposing Behaviors with Ensembles of Piriform Neurons. Cell. 2011; 146:1004–1015. [PubMed: 21925321]
20. Meissner-Bernard C, Dembitskaya Y, Venance L, Fleischmann A. Encoding of Odor Fear Memories in the Mouse Olfactory Cortex. Curr Biol. 2019; 29:367–380.e4. [PubMed: 30612908]
21. Sacco T, Sacchetti B. Role of Secondary Sensory Cortices in Emotional Memory Storage and Retrieval in Rats. Science. 2010; 329:649–656. [PubMed: 20689011]
22. Hennequin G, Agnes EJ, Vogels TP. Inhibitory Plasticity: Balance, Control, and Codependence. Annu Rev Neurosci. 2017; 40:557–579. [PubMed: 28598717]
23. Poo C, Isaacson JS. Odor Representations in Olfactory Cortex: "Sparse" Coding, Global Inhibition, and Oscillations. Neuron. 2009; 62:850–861. [PubMed: 19555653]
24. Mueller T, Dong Z, Berberoglu MA, Guo S. The dorsal pallium in zebrafish, Danio rerio (Cyprinidae, Teleostei). Brain Res. 2011; 1381:95–105. [PubMed: 21219890]
25. Miyasaka N, et al. Olfactory projectome in the zebrafish forebrain revealed by genetic single-neuron labelling. Nat Commun. 2014; 5:3639. [PubMed: 24714622]
26. Blumhagen F, et al. Neuronal filtering of multiplexed odour representations. Nature. 2011; 479:493–498. [PubMed: 22080956]
27. Yaksi E, von Saint Paul F, Niessing J, Bundschuh ST, Friedrich RW. Transformation of odor representations in target areas of the olfactory bulb. Nat Neurosci. 2009; 12:474–482. [PubMed: 19305401]
28. Jacobson GA, Rupprecht P, Friedrich RW. Experience-Dependent Plasticity of Odor Representations in the Telencephalon of Zebrafish. Curr Biol. 2018; 28:1–14.e3. [PubMed: 29249662]
29. Rupprecht P, Friedrich RW. Precise Synaptic Balance in the Zebrafish Homolog of Olfactory Cortex. Neuron. 2018; 100:669–683.e5. [PubMed: 30318416]
30. Friedrich RW, Laurent G. Dynamic Optimization of Odor Representations by Slow Temporal Patterning of Mitral Cell Activity. Science. 2001; 291:889–894. [PubMed: 11157170]
31. Miklavc P, Valentinčič T. Chemotopy of Amino Acids on the Olfactory Bulb Predicts Olfactory Discrimination Capabilities of Zebrafish Daniorerio. Chem Senses. 2012; 37:65–75. [PubMed: 21778519]
32. Vitebsky A, Reyes R, Sanderson MJ, Michel WC, Whitlock KE. Isolation and characterization of the laure olfactory behavioral mutant in the zebrafish, Danio rerio. Dev Dyn. 2005; 234:229–242. [PubMed: 16086331]
33. Namekawa I, Moenig NR, Friedrich RW. Rapid olfactory discrimination learning in adult zebrafish. Exp Brain Res. 2018; :1–11. DOI: 10.1007/s00221-018-5352-x
34. Sturgill JF, Isaacson JS. Somatostatin cells regulate sensory response fidelity via subtractive inhibition in olfactory cortex. Nat Neurosci. 2015; 18:531–535. [PubMed: 25751531]
35. Aso Y, et al. Mushroom body output neurons encode valence and guide memory-based action selection in Drosophila. eLife. 2014; 3:e04580. [PubMed: 25535794]
36. Gradinaru V, et al. Molecular and Cellular Approaches for Diversifying and Extending Optogenetics. Cell. 2010; 141:154–165. [PubMed: 20303157]
37. Satou C, et al. Transgenic tools to characterize neuronal properties of discrete populations of zebrafish neurons. Development. 2013; 140:3927–3931. [PubMed: 23946442]
38. Mueller T, Guo S. The distribution of GAD67-mRNA in the adult zebrafish (teleost) forebrain reveals a prosomeric pattern and suggests previously unidentified homologies to tetrapods. J Comp Neurol. 2009; 516:553–568. [PubMed: 19673006]
39. Miura K, Mainen ZF, Uchida N. Odor Representations in Olfactory Cortex: Distributed Rate Coding and Decorrelated Population Activity. Neuron. 2012; 74:1087–1098. [PubMed: 22726838]
40. Kadohisa M, Wilson DA. Separate encoding of identity and similarity of complex familiar odors in piriform cortex. Proc Natl Acad Sci. 2006; 103:15206–15211. [PubMed: 17005727]

41. Calu DJ, Roesch MR, Stalnaker TA, Schoenbaum G. Associative Encoding in Posterior Piriform Cortex during Odor Discrimination and Reversal Learning. Cereb Cortex. 2007; 17:1342–1349. [PubMed: 16882682]
42. Howard JD, Plailly J, Grueschow M, Haynes J-D, Gottfried JA. Odor quality coding and categorization in human posterior piriform cortex. Nat Neurosci. 2009; 12:932–938. [PubMed: 19483688]
43. Blake DT, Strata F, Churchland AK, Merzenich MM. Neural correlates of instrumental learning in primary auditory cortex. Proc Natl Acad Sci. 2002; 99:10114–10119. [PubMed: 12119383]
44. Poort J, et al. Learning Enhances Sensory and Multiple Non-sensory Representations in Primary Visual Cortex. Neuron. 2015; 86:1478–1490. [PubMed: 26051421]
45. Rutkowski RG, Weinberger NM. Encoding of learned importance of sound by magnitude of representational area in primary auditory cortex. Proc Natl Acad Sci U S A. 2005; 102:13664–13669. [PubMed: 16174754]
46. Yan Y, et al. Perceptual training continuously refines neuronal population codes in primary visual cortex. Nat Neurosci. 2014; 17:1380–1387. [PubMed: 25195103]
47. Secundo L, Snitz K, Sobel N. The perceptual logic of smell. Curr Opin Neurobiol. 2014; 25:107–115. [PubMed: 24440370]
48. Hige T, Aso Y, Rubin GM, Turner GC. Plasticity-driven individualization of olfactory coding in mushroom body output neurons. Nature. 2015; 526:258–262. [PubMed: 26416731]
49. Séjourné J, et al. Mushroom body efferent neurons responsible for aversive olfactory memory retrieval in *Drosophila* . Nat Neurosci. 2011; 14:903–910. [PubMed: 21685917]
50. Khan AG, et al. Distinct learning-induced changes in stimulus selectivity and interactions of GABAergic interneuron classes in visual cortex. Nat Neurosci. 2018; 21:851–859. [PubMed: 29786081]
51. Cocco A, et al. Characterization of the γ-aminobutyric acid signaling system in the zebrafish (Danio rerio Hamilton) central nervous system by reverse transcription-quantitative polymerase chain reaction. Neuroscience. 2017; 343:300–321. [PubMed: 27453477]
52. Kwan KM, et al. The Tol2kit: A multisite gateway-based construction kit forTol2 transposon transgenesis constructs. Dev Dyn. 2007; 236:3088–3099. [PubMed: 17937395]
53. Distel M, Wullimann MF, Köster RW. Optimized Gal4 genetics for permanent gene expression mapping in zebrafish. Proc Natl Acad Sci. 2009; 106:13365–13370. [PubMed: 19628697]
54. Kawakami K, et al. A Transposon-Mediated Gene Trap Approach Identifies Developmentally Regulated Genes in Zebrafish. Dev Cell. 2004; 7:133–144. [PubMed: 15239961]
55. Suster ML, Sumiyama K, Kawakami K. Transposon-mediated BAC transgenesis in zebrafish and mice. BMC Genomics. 2009; 10:477. [PubMed: 19832998]
56. Asakawa K, et al. Genetic dissection of neural circuits by Tol2 transposon-mediated Gal4 gene and enhancer trapping in zebrafish. Proc Natl Acad Sci. 2008; 105:1255–1260. [PubMed: 18202183]
57. Mathieson WB, Maler L. Morphological and electrophysiological properties of a novel in vitro preparation: the electrosensory lateral line lobe brain slice. J Comp Physiol A. 1988; 163:489–506. [PubMed: 3184011]
58. Wullimann, M. Neuroanatomy of the zebrafish brain: a topological atlas. Birkhäuser Verlag; 1996.
59. Zhu P, Fajardo O, Shum J, Schärer Y-PZ, Friedrich RW. High-resolution optical control of spatiotemporal neuronal activity patterns in zebrafish using a digital micromirror device. Nat Protoc. 2012; 7:1410–1425. [PubMed: 22743832]
60. Pologruto TA, Sabatini BL, Svoboda K. ScanImage: flexible software for operating laser scanning microscopes. Biomed Eng Online. 2003; 2:13. [PubMed: 12801419]
61. Suter BA, et al. Ephus: multipurpose data acquisition software for neuroscience experiments. Front Neural Circuits. 2010; 4:100. [PubMed: 21960959]
62. Valentinčič T, Metelko J, Ota D, Pirc V, Blejec A. Olfactory Discrimination of Amino Acids in Brown Bullhead Catfish. Chem Senses. 2000; 25:21–29. [PubMed: 10667990]
63. Duguid I, Branco T, London M, Chadderton P, Häusser M. Tonic Inhibition Enhances Fidelity of Sensory Information Transmission in the Cerebellar Cortex. J Neurosci. 2012; 32:11132–11143. [PubMed: 22875944]

64. Vinje WE, Gallant JL. Sparse Coding and Decorrelation in Primary Visual Cortex During Natural Vision. Science. 2000; 287:1273–1276. [PubMed: 10678835]

65. Bathellier B, Buhl DL, Accolla R, Carleton A. Dynamic Ensemble Odor Coding in the Mammalian Olfactory Bulb: Sensory Information at Different Timescales. Neuron. 2008; 57:586–598. [PubMed: 18304487]

Europe PMC Funders Author Manuscripts

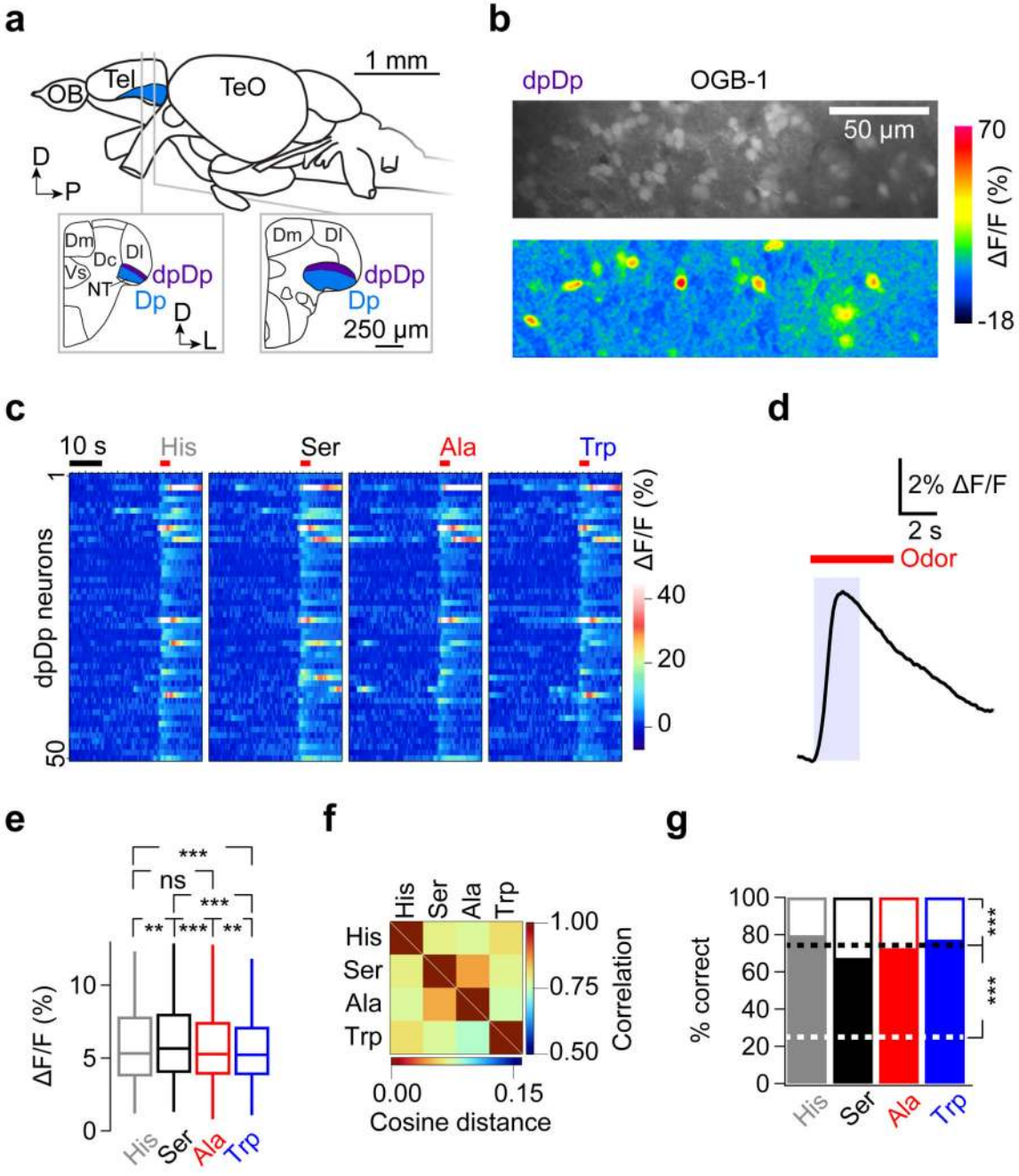

Fig. 1. Odor representations in dorsal posterior Dp (dpDp) in naïve fish

a. Location of dpDp (lateral view of the zebrafish brain and two coronal cross-sections) OB: olfactory bulb; Tel: telencephalon; TeO: optic tectum; Dc: central zone of the dorsal telencephalon; Dl: lateral zone of the dorsal telencephalon; Dm: medial zone of the dorsal telencephalon; Dp: posterior zone of the dorsal telencephalon; dpDp: dorsal-posterior Dp; NT: Nucleus taeniae; Vs: supracommissural nucleus of the ventral telencephalon. Scale bars represent approximations. D: dorsal; P: posterior; L: lateral.

Europe PMC Funders Author Manuscripts

b. dpDp neurons loaded with OGB-1 (top) and Ca^{2+} signals (bottom) evoked in the same field of view by odor stimulation (Ala, single trial).

c. Odor-evoked Ca^{2+} signals of 50 randomly selected dpDp neurons before, during, and after stimulation with four different amino acid odors (10^{-4} M; average of three trials each).

d. Ca^{2+} signal averaged over all trials (n = 3), odors (n = 4), and neurons (n = 1790, from N = 13 animals). Gray shading shows s.e.m.. Red bar indicates approximate duration of odor stimulation and blue shaded area depicts the 2 s time window used for most analyses.

e. Amplitude of Ca^{2+} signals evoked by different odors (median ± s.d.). Pairwise odor comparisons (paired *t* tests, two-sided, n = 1790 neurons from N = 13 animals, df = 1789): His vs Ser, $t = -3.70$, p = 0.0002; His vs Ala, $t = 0.36$, p = 0.72; His vs Trp, $t = 3.94$, p = $8x10^{-5}$; Ser vs Ala, $t = -4.37$, p = $1x10^{-5}$; Ser vs Trp, $t = 7.05$, p = $3x10^{-12}$; Ala vs Trp, $t = 3.74$, p = 0.0002. Box plot: center line, median; box limits, interquartile range; whiskers, standard deviation.

f. Pattern similarity matrix showing cosine distance (below diagonal) and Pearson correlation (above diagonal) between trial-averaged activity patterns evoked by different odor stimuli (average over N = 13 animals). Diagonal values were set to zero (cosine distance) or one (Pearson correlation).

g. Classification of odor identity by template matching of activity vectors. Fills show percentage of correctly decoded odors using a fixed population size of 95 neurons. White dashed line indicates chance level (25 %; McNemar test, n = 156 trials, df = 1, $X^2 = 74.01$, p < 10^{-16}), and black dashed line shows mean classification success, averaged over all four odors (McNemar test for comparison against 100% correct, $X^2 = 39.02$, p = $4x10^{-10}$).

Europe PMC Funders Author Manuscripts

Europe PMC Funders Author Manuscripts

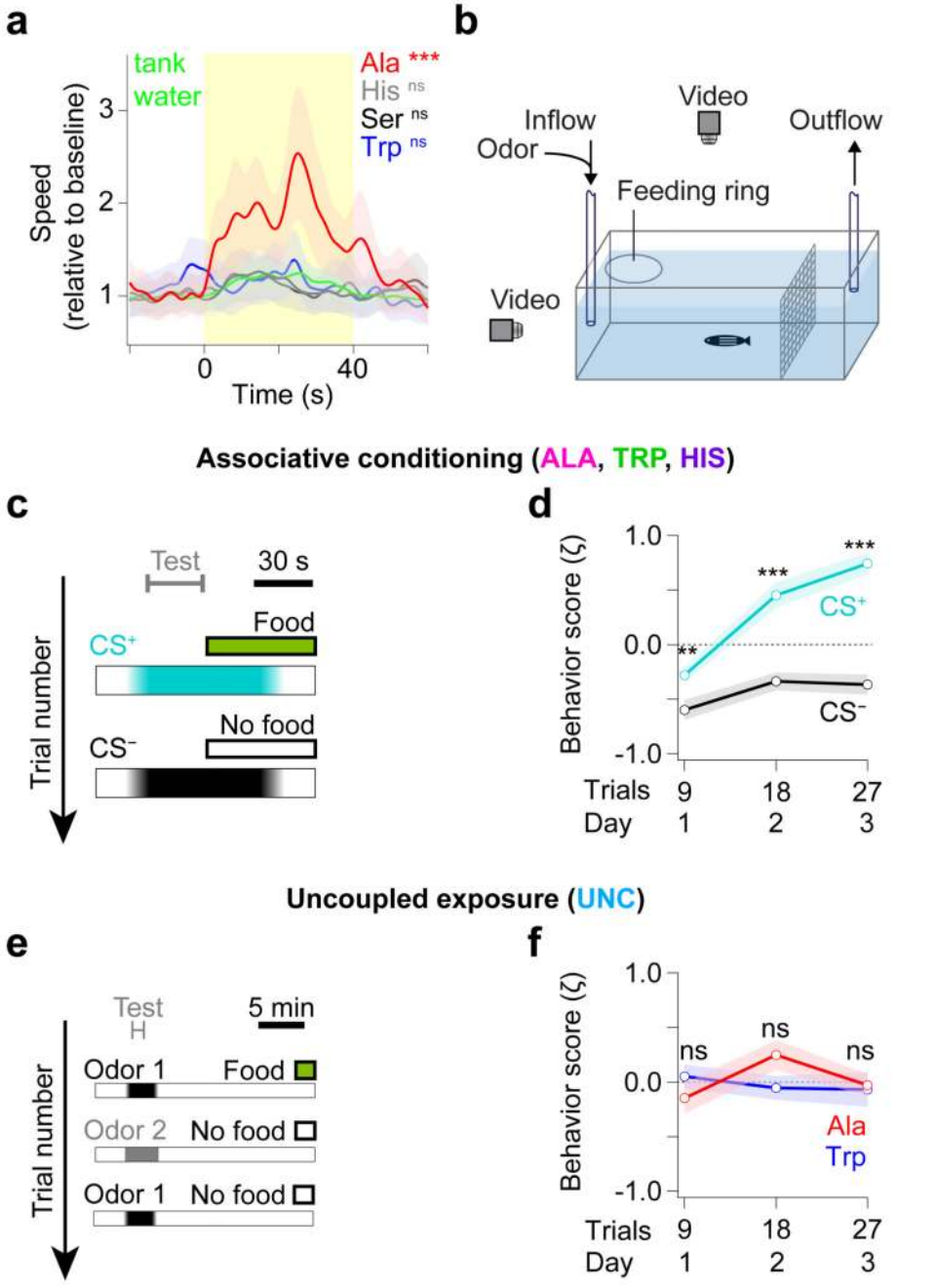

Fig. 2. Innate odor preference and associative olfactory conditioning

a. Innate behavioral responses to the four amino acid odors used in this study and tank water as control (green). Curves show mean swimming speed (boxcar smoothed) normalized to pre-application baseline. Shading shows s.e.m.. Mean swimming speed averaged over 40 s (yellow rectangle) was significantly modulated by odor application (Kruskal-Wallis test, N = 141, df = 4, H = 15.44, p = 0.003), differing from tank water (N = 71 animals) for Ala (N = 16, Q = −3.59, p = 0.0007) but not for other odors (His: N = 20, Q = 0.10, p = 1; Ser: N = 20, Q = 0.16, p = 1; Trp: N = 14, Q = 0.69, p = 0.93).

Europe PMC Funders Author Manuscripts

b. Schematic of setup for associative olfactory conditioning.

c. Schedule for associative conditioning. The CS^+, but not the CS^-, was followed by a food reward. The behavioral response was measured during the first 30 s between odor onset and food delivery ('Test').

d. Mean learning curves. ζ is a composite score combining multiple components of appetitive behavior. Lines and shading show the mean (± s.e.m.) of ζ for the first three days of training (nine trials per day). Comparisons between CS^+ and CS^- (Wilcoxon signed rank test, two-sided, N = 43 animals [2 fish without data on day 1], ALA, TRP, and HIS): day 1, N = 41, T = 206, p = 0.003; day 2, N = 43, T = 133, $p = 1x10^{-5}$; day 3, N = 43, T = 42, $p = 3x10^{-9}$.

e. Schedule for uncoupled odor exposure. The same odor stimuli as for associative conditioning (Ala and Trp) were applied 15 min prior to food presentation, which occurred with a probability of 50 % on each trial, independent of the odor (Online Methods).

f. Mean ζ-scores for Ala and Trp in UNC fish. Lines and shading show the mean (± s.e.m.). No systematic differences in appetitive responses to Ala and Trp were observed (Wilcoxon signed rank test, two-sided, N = 12 animals): day 1, T = 25, p = 0.30; day 2, T = 20, p= 0.15; day 3, T = 33, p = 0.68.

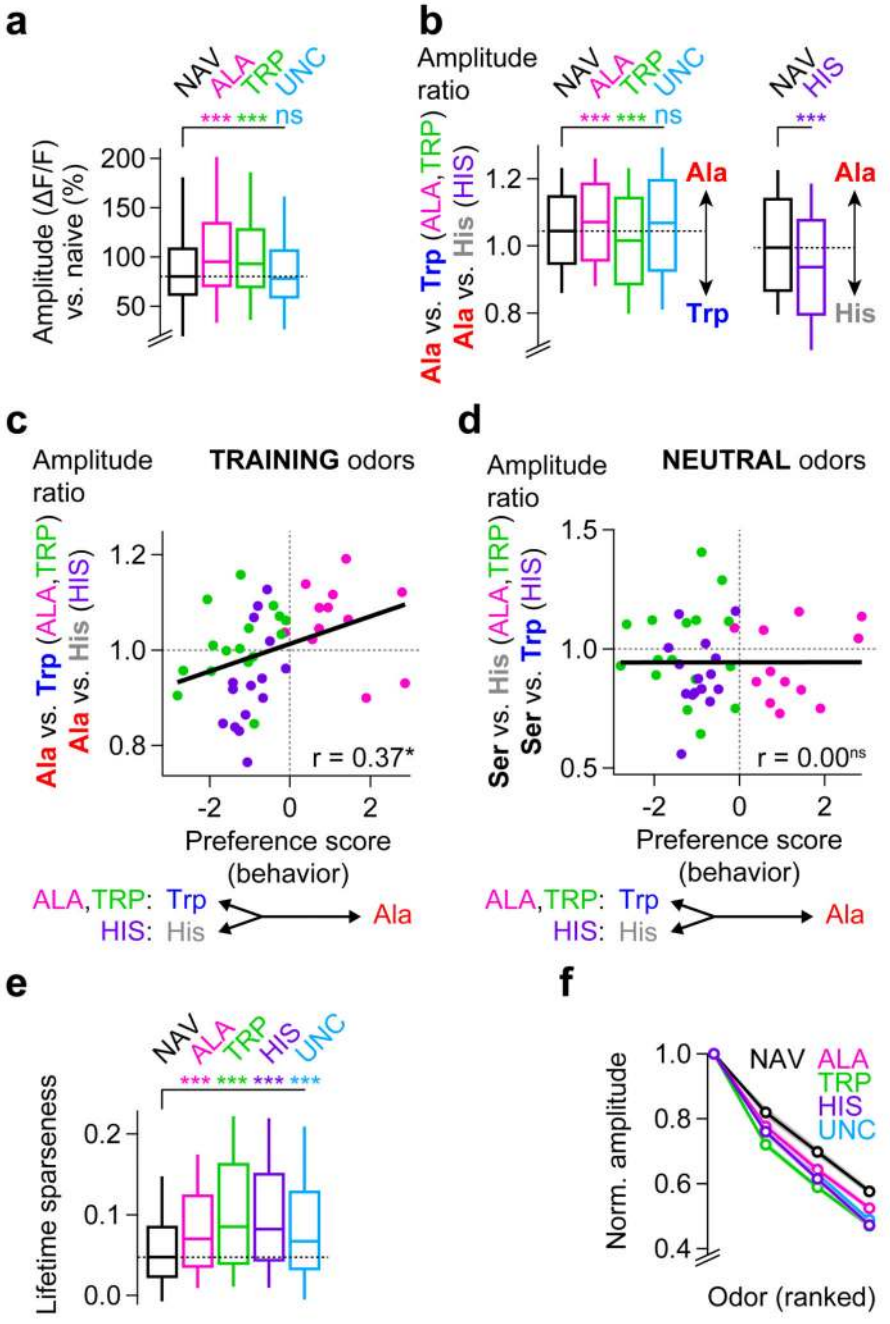

Fig. 3. Learning- and experience-dependent enhancement of odor responses in dpDp

a. Mean odor-evoked response amplitude averaged over all neuron-odor pairs, expressed as percentage of mean amplitude in NAV fish. Responses of ALA and TRP fish were significantly higher than responses of NAV fish (Kruskal-Wallis test, n = 5654, df = 3, H = 155.69, $p < 10^{-15}$). Non-parametric multiple comparisons against NAV (n = 1262): ALA, Q = −9.03, $p < 10^{-15}$, n = 1591; TRP, Q = −7.62, $p = 5x10^{-14}$, n = 1839; UNC, Q = 1.44, p = 0.30, n = 962. Box plot: center line, median; box limits, interquartile range; whiskers, standard deviation.

b. Ratio of Ala/Trp response amplitudes (Kruskal-Wallis test with NAV, ALA, TRP, UNC: n = 6423, df = 3, H = 85.33, $p < 10^{-15}$) or Ala/His response amplitudes (Wilcoxon-Mann-Whitney test, two-sided: NAV, n = 528, HIS, n = 2040, U = 444'188, $p = 4x10^{-10}$) differed between experimental groups. Non-parametric multiple comparisons against NAV (n = 1262), two-sided: ALA, Q = −3.62, p = 0.0006, n = 1591; TRP, Q = 4.17, $p = 6x10^{-5}$, n = 2162; UNC, Q = -2.01, p = 0.09, n = 1408. Results show that associative conditioning shifted relative response amplitudes towards the CS^+. Box plot: as in (**a**).

c. Relative response amplitudes to training odors (Ala vs Trp or His) were correlated to behavioral odor preference in individual fish (ALA, TRP, and HIS; color code as in **b**). Pearson correlation: r = 0.37 (N = 43 animals, *t* test of null hypothesis of r = 0, two-sided, df = 41, *t* = 2.54, p = 0.02). Kendall's rank correlation: $\tau = 0.31$ (test of null hypothesis of $\tau = 0$ using a normal approximation, two-sided, z = 2.90, p = 0.004).

d. Relative response amplitudes to neutral odors (Ser vsHis or Trp) were not correlated to behavioral odor preference. Pearson correlation: r = 0.00 (*t* test of null hypothesis of r = 0, two-sided, *t* = 0.004, p = 1). Kendall's rank correlation: $\tau = -0.03$ (test of null hypothesis of $\tau = 0$ using a normal approximation, two-sided, z = –0.32, p = 0.75). N as in (**c**).

e. Lifetime sparseness was increased after associative conditioning and uncoupled odor exposure (Kruskal-Wallis test, n = 8991, df = 4, H = 366.19, $p < 10^{-15}$). Non-parametric multiple comparisons against NAV (n = 1790), two-sided: ALA, Q = –9.95, $p < 10^{-15}$, n = 1591; TRP, Q = –16.76, $p < 10^{-15}$, n = 2162; HIS, Q = –16.72, $p < 10^{-15}$, n = 2040; UNC, Q = –9.72, $p < 10^{-15}$, n = 1408. Box plot: as in (**a**).

f. Mean tuning curves (line), constructed by rank-ordering of odor responses in each neuron. Shaded areas show s.e.m.. The slope of individual tuning curves was significantly increased (Kruskal-Wallis test, n = 6202, df = 4, H = 314.94, $p < 10^{-15}$; non-parametric comparison against NAV, n = 1322 neurons with trial-averaged responses to at least one odor, two-sided: ALA, Q = 8.47, $p < 10^{-15}$, n = 1325; TRP, Q = 14.83, $p < 10^{-15}$, n = 1603; HIS, Q = 15.52, $p < 10^{-15}$, n = 992; UNC, Q = 9.43, $p < 10^{-16}$, n = 960).

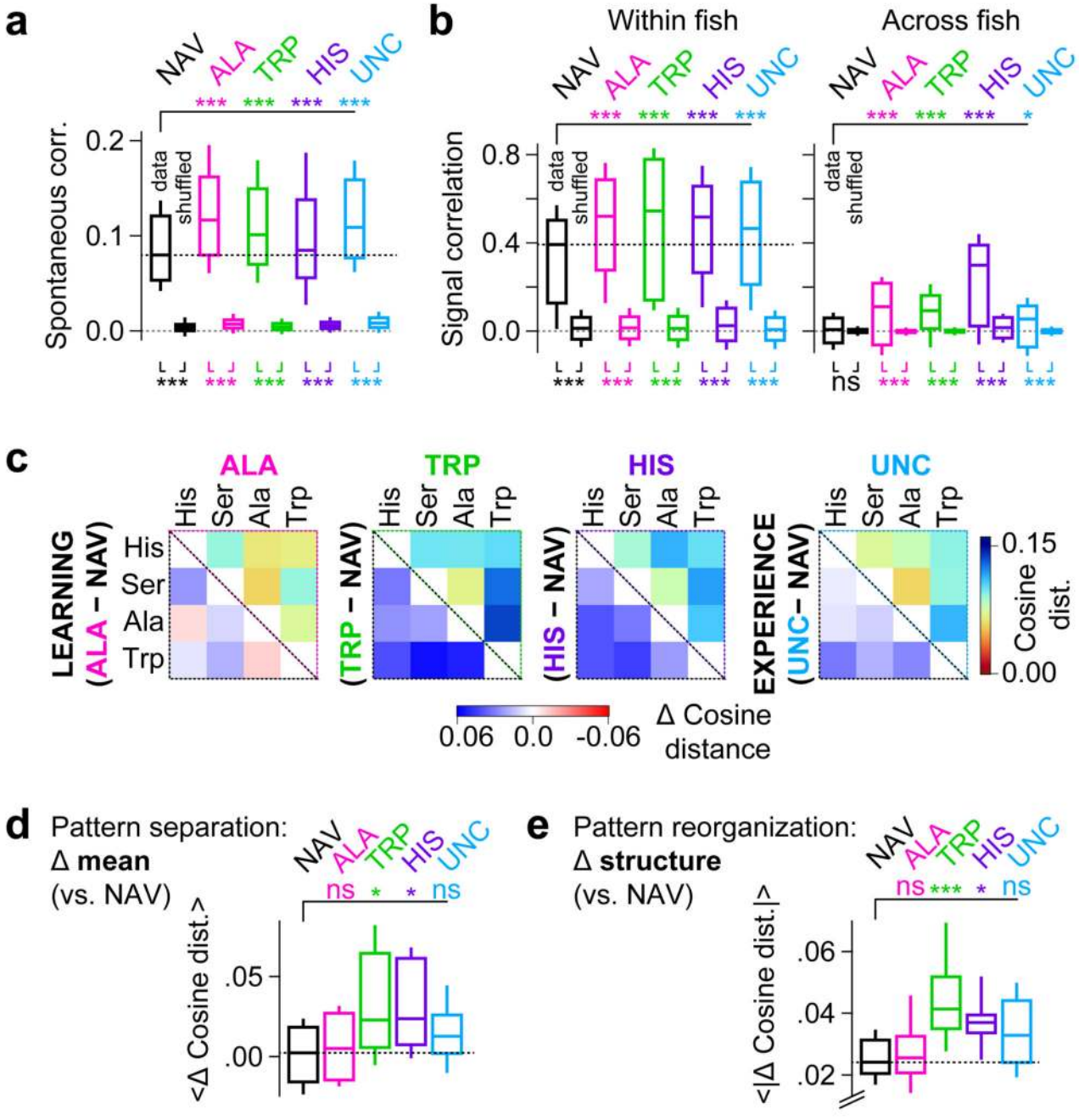

Fig. 4. Experience strengthens pairwise correlations and modifies neuronal population activity in dpDp

a. Correlation of spontaneous activity after associative conditioning and uncoupled odor exposure was significantly higher than in NAV fish ('data'; Kruskal-Wallis test, n = 8991, df = 4, H = 431.64, $p < 10^{-15}$). Non-parametric multiple comparisons against NAV, two-sided: ALA, Q = –17.33, $p < 10^{-15}$; TRP, Q = –12.43, $p < 10^{-15}$; HIS, Q = –4.88, $p = 2x10^{-6}$; UNC, Q = –14.76, $p < 10^{-15}$. Shuffling of time bins abolished correlations ('data' vs 'shuffled'; paired *t* test, two-sided, df = n-1: NAV, $t = 79.16$, $p < 10^{-300}$; ALA, $t = 72.86$, p <

Europe PMC Funders Author Manuscripts

10^{-300}; TRP, $t = 80.06$, $p < 10^{-300}$; HIS, $t = 58.90$, $p < 10^{-300}$; UNC, $t = 76.33$, $p < 10^{-300}$). Number of neurons as in Fig. 3e. Box plot: center line, median; box limits, interquartile range; whiskers, standard deviation.

b. Correlation of odor tuning curves (signal correlation) after associative conditioning and uncoupled odor exposure was significantly higher than in NAV fish, both within the same fish (left; Kruskal-Wallis test, n = 6202, df = 4, H = 332.18, $p < 10^{-15}$) and across fish (right; H = 785.84, $p < 10^{-15}$). Only neurons that responded to at least one odor were included in this analysis. Non-parametric multiple comparisons against NAV within fish (n = 1322), two-sided: ALA, Q = –14.18, $p < 10^{-15}$, n = 1325; TRP, Q = –16.86, $p < 10^{-15}$, n = 1603; HIS, Q = –12.14, $p < 10^{-15}$, n = 992; UNC, Q = –10.45, $p < 10^{-15}$, n = 960. Across fish (n = 1322), two-sided: ALA, Q = –14.38, $p < 10^{-15}$; TRP, Q = –14.95, $p < 10^{-15}$; HIS, Q = –26.57, $p < 10^{-15}$; UNC, Q = –5.31, $p = 2x10^{-7}$. Correlations were abolished after shuffling of stimulus labels ('data' vs 'shuffled', paired *t* test, two-sided, df = n-1). Within fish: NAV, $t = 36.18$, $p = 9x10^{-200}$; ALA, $t = 48.93$, $p = 3x10^{-299}$; TRP, $t = 48.68$, $p = 4x10^{-318}$; HIS, $t = 39.17$, $p = 2x10^{-203}$; UNC, $t = 38.59$, $p = 2x10^{-197}$. Across fish: NAV, $t = –0.14$, $p = 0.89$; ALA, $t = 14.28$, $p = 4x10^{-43}$; TRP, $t = 19.55$, $p = 2x10^{-76}$; HIS, $t = 19.55$, $p = 2x10^{-95}$; UNC, $t = 4.57$, $p = 5x10^{-6}$. Box plot: as in (**a**).

c. Effects of experience on the cosine distance between odor-evoked activity patterns. The triangles above the diagonal contain distance matrices averaged over individuals in each training group. The triangles below the diagonal contain the difference between each matrix and the distance matrix of NAV fish (Fig. 1f). Increases (decreases) in pattern distance are depicted by blue (red) colors. Number of animals as in (**d**).

d. Mean pairwise cosine distance of activity patterns ('pattern separation') was increased in TRP and HIS fish (Kruskal-Wallis test, N = 68 animals, df = 4, H = 10.71, p = 0.03). Non-parametric multiple comparisons against NAV, two-sided: ALA, Q = –0.51, p = 0.96, N = 12; TRP, Q = –2.55, p = 0.02, N = 16; HIS, Q = –2.59, p = 0.02, N = 15; UNC, Q = –1.38, p = 0.33, N = 12. Box plot: as in (**a**).

e. Mean absolute difference of centered distance matrices to the mean matrix of NAV fish was increased in TRP and HIS fish (Kruskal-Wallis test, H = 17.84, p = 0.0008). This measure quantifies the reorganization of the structure of distance matrices (Online Methods) relative to the mean NAV matrix, even in the absence of a change in mean pattern distance. Non-parametric multiple comparisons against NAV, two-sided: ALA, Q = –0.49, p = 0.97; TRP, Q = –3.71, p = 0.0004; HIS, Q = –2.50, p = 0.02; UNC, Q = –1.65, p = 0.20. Number of animals and df as in (**d**). Box plot: as in (**a**).

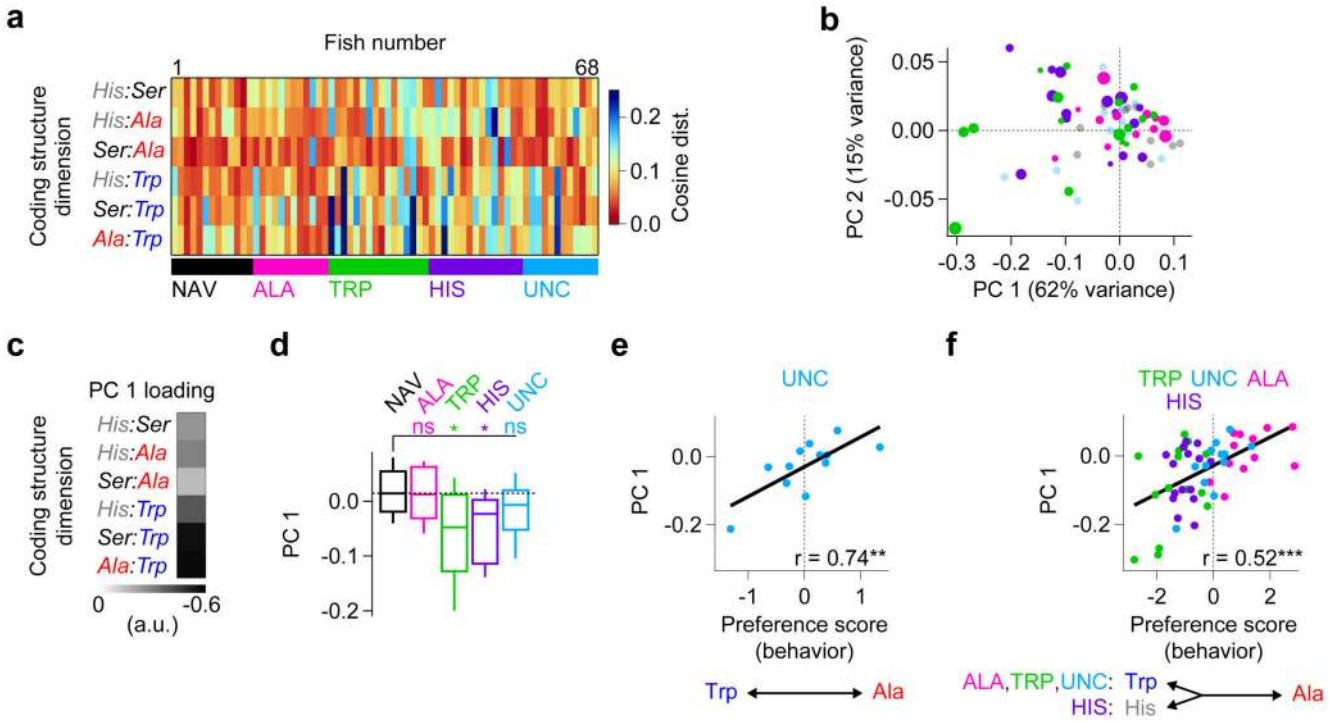

Fig. 5. Mapping odor space onto a valence axis

a. Coding structures of all fish (N = 68 animals) from all five experimental groups. Each column (observation) is one coding structure. Rows (variables) represent cosine distances between activity patterns evoked by different odor pairs.

b. Projection of coding structures of all fish onto the first two principal components. Each plot symbol represents one fish. Colors show association of each coding structure with the experimental group. For ALA, TRP, and HIS fish, larger marker size indicates higher behavioral discrimination score. Number of animals as in (**a**).

c. PC 1 loadings on the six coding structure dimensions. Number of animals as in (**a**).

d. Mean PC 1 scores differed significantly between experimental groups (Kruskal-Wallis test, H = 10.01, p = 0.04; same data as in **b**). PC 1 scores in TRP and HIS fish were significantly more negative than in NAV fish. Non-parametric multiple comparisons against NAV: ALA, Q = 0.43, p = 0.98; TRP, Q = 2.43, p = 0.03; HIS, Q = 2.49, p = 0.03; UNC, Q = 1.44, p = 0.30. Number of animals and df as in Fig. 4d. Box plot: center line, median; box limits, interquartile range; whiskers, standard deviation.

e. Significant correlation between PC 1 score and behavioral odor preference in UNC fish. Pearson correlation: r = 0.74 (N = 12, *t* test of null hypothesis of r = 0, two-sided, df = 10, $t = 3.50$, p = 0.006). Kendall's rank correlation: $\tau = 0.58$ (test of null hypothesis of $\tau = 0$ using a normal approximation, two-sided, z = 2.61, p = 0.009).

f. Significant correlation between PC 1 score and behavioral odor preference across all training groups. Pearson correlation: r = 0.52 (N = 55, *t* test of null hypothesis of r = 0, two-sided, df = 53, $t = 4.48$, $p = 4 \times 10^{-5}$). Kendall's rank correlation: $\tau = 0.35$ (test of null hypothesis of $\tau = 0$ using a normal approximation, two-sided, z = 3.72, p = 0.0002).

Europe PMC Funders Author Manuscripts

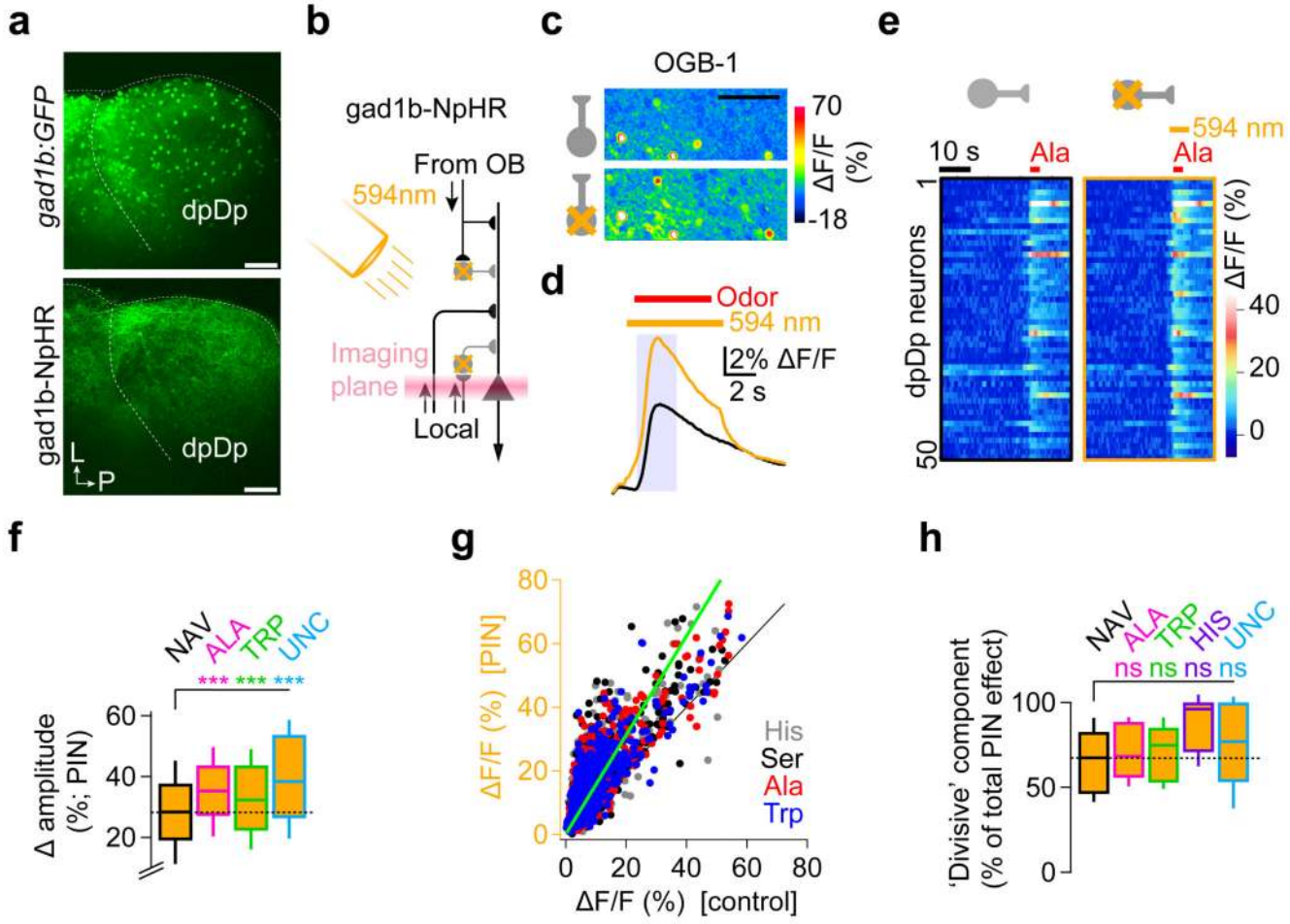

Fig. 6. Experience-dependent enhancement of inhibition in dpDp

a. Expression of GFP in Tg(*gad1b:GFP*) and of eNpHR3.0YFP in Tg(*gad1b:Gal4, UAS:eNpHR3.0YFP*) fish. Images are maximum intensity projection of multiphoton image stacks covering the dorso-ventral extent of Dp, including dpDp, over which odor-evoked activity was measured (approximately 70 μm). See also Supplementary Fig. 6a. Scale bars: 50μm; L: lateral; P: posterior. The experiment was independently repeated three times (*gad1b:GFP*), and 68 times (gad1b-NpHR), respectively, with similar results.

b. Scheme illustrating expression of eNpHR3.0YFP in a broad spectrum of interneurons in dpDp, hyperpolarization of interneurons by orange light (594 nm) through an optical fiber, and simultaneous two-photon Ca^{2+} imaging.

c. Example of odor-evoked Ca^{2+} signals in dpDp under control conditions (top) and during PIN (bottom). Scale bar: 50μm.

d. Odor-evoked Ca^{2+} signal averaged over all neurons, trials and odors in NAV fish under control conditions (black; same as in Fig. 1d) and during PIN (orange). Shadings show s.e.m. (n as in Fig. 1d). Red bar indicates approximate duration of odor stimulation; orange bar depicts light exposure.

e. Spontaneous and odor-evoked Ca^{2+} signals in 50 randomly selected dpDp neurons under control conditions (left) and during PIN (right; Ala, average of n = 3 trials). Red bar approximates duration of odor stimulus (Ala).

f. The PIN-mediated increase in odor response amplitude, which reflects the strength of odor-evoked inhibition, was increased after associative conditioning and uncoupled odor exposure (Kruskal-Wallis test, n = 5654, df = 3, H = 250.75, $p < 10^{-15}$). Non-parametric comparisons to NAV (n = 1262), two-sided: ALA, Q = –11.82, $p < 10^{-15}$, n = 1591; TRP, Q = –7.47, $p = 2x10^{-13}$, n = 1893; UNC, Q = –14.72, $p < 10^{-15}$, n = 962. Amplitude change is expressed in percent suppression of PIN amplitude. Box plot: center line, median; box limits, interquartile range; whiskers, standard deviation.

g. Amplitudes of individual odor responses under control conditions (x-axis) and during PIN (y-axis) in NAV fish. Each data point represents one neuron-odor pair (n = 7160 from N = 13 animals). Green line is a linear fit (total least squares) indicating primarily divisive inhibition. Responses to different odors are shown in different colors; no obvious differences were observed between responses to different odors.

h. The relative contribution of divisive and subtractive effects of inhibition were not modulated by odor experience (Kruskal-Wallis test, N = 68, df = 4, H = 4.64, p = 0.33). In each fish, a linear function was fitted to all responses of individual neurons to determine the relative contribution of the offset and the slope of the fit, respectively, to the total PIN-induced disinhibition. The divisive component dominated in all groups. Non-parametric multiple comparisons against NAV, two-sided: ALA, Q = –0.61, p = 0.93; TRP, Q = –0.38, p = 0.99; HIS, Q = –1.91, p = 0.11; UNC, Q = –1.19, p = 0.47. Number of animals as in Fig. 4d. Box plot: as in (**f**).

Europe PMC Funders Author Manuscripts

Europe PMC Funders Author Manuscripts

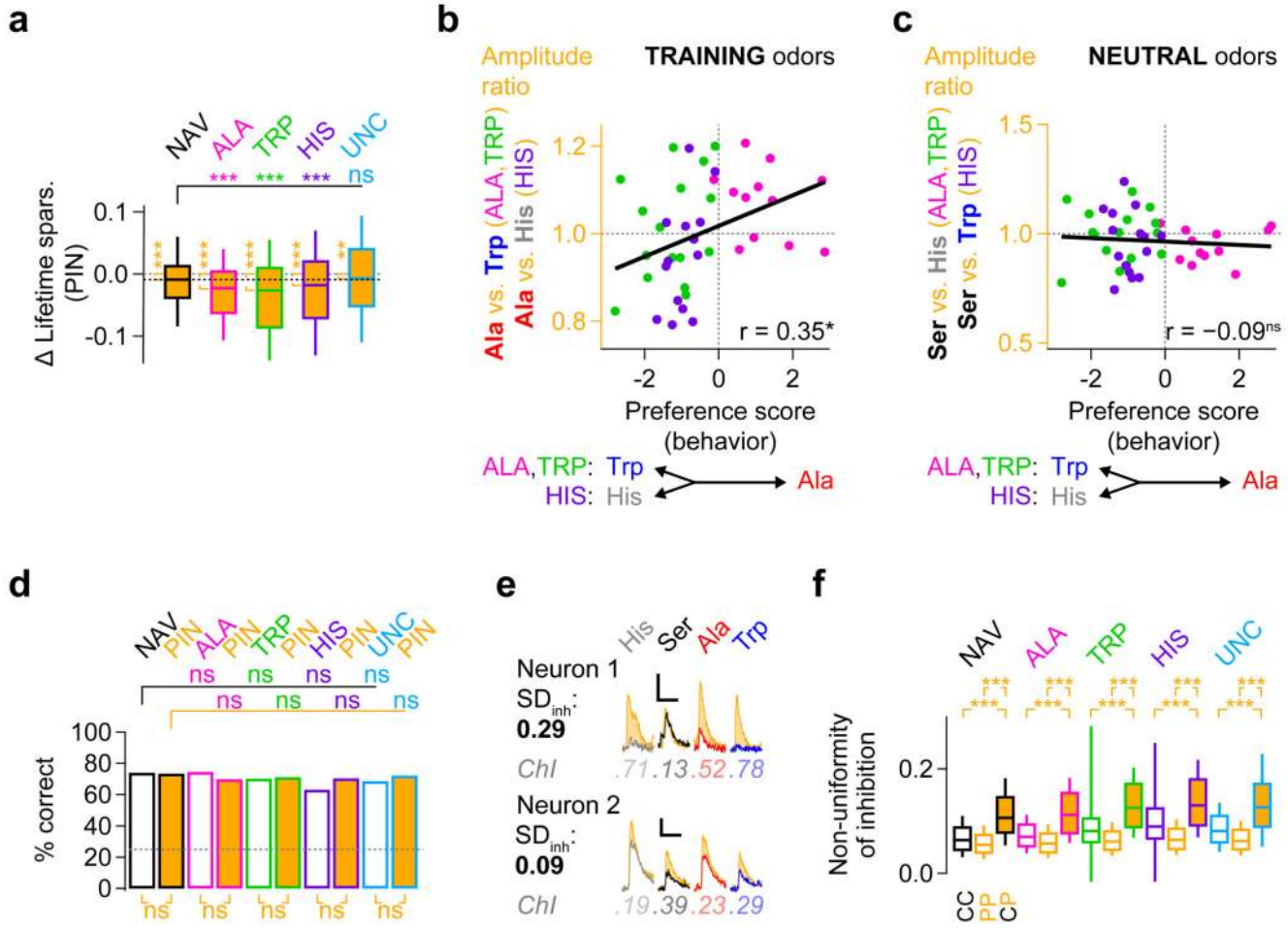

Fig. 7. Non-uniform effects of inhibition in dpDp

a. PIN decreased tuning sharpness and this effect was enhanced after associative conditioning. Box plots quantify differences in lifetime sparseness of the same neurons under control conditions and during PIN (Kruskal-Wallis test, n = 8991, df = 4, H = 167.75, $p < 10^{-15}$). Comparisons of PIN vs control (paired *t* test, two-sided): NAV, *t* = 7.09, p = $2x10^{-12}$; ALA, *t* = 18.12, p = $8x10^{-67}$; TRP, *t* = 20.09, p = $2x10^{-82}$; HIS, *t* = 13.74, p = $4x10^{-41}$; UNC, *t* = 2.92, p = 0.004. Non-parametric multiple comparisons against NAV, two-sided: ALA, Q = 7.51, p = $1x10^{-13}$; TRP, Q = 9.30, $p < 10^{-15}$; HIS, Q = 4.87, p = $2x10^{-6}$; UNC, Q = –1.68, p = 0.18. Number of neurons and df as in Fig. 3e. Box plot: center line, median; box limits, interquartile range; whiskers, standard deviation.

b. Relative response amplitudes to training odors (Ala vs Trp or His) remained correlated to behavioral odor preference in individual ALA, TRP, and HIS fish during PIN. Pearson correlation: r = 0.35 (*t* test of null hypothesis of r = 0, two-sided, *t* = 2.40, p = 0.02). Kendall's rank correlation: $\tau = 0.30$ (test of null hypothesis of $\tau = 0$ using a normal approximation, two-sided, z = 2.79, p = 0.005). Number of animals and df as in Fig. 3c.

c. Relative response amplitudes to neutral odors (Ser vs His or Trp) remained uncorrelated to behavioral odor preference in individual ALA, TRP, and HIS fish during PIN. Pearson correlation: r = –0.09 (*t* test of null hypothesis of r = 0, two-sided, *t* = –0.56, p = 0.58).

Kendall's rank correlation: $\tau = -0.07$ (test of null hypothesis of $\tau = 0$ using a normal approximation, two-sided, z = –0.68, p = 0.49). Number of animals and df as in Fig. 3c.
d. PIN did not affect odor identification by template matching. Bars show percentage of correct odor identifications under control conditions (open bars) and during PIN (orange bars). Control vs PIN comparisons, McNemar test, df = 1: NAV, $X^2 = 0$, p = 1, n = 156 trials; ALA, $X^2 = 0.25$, p = 0.62, n = 144; TRP, $X^2 = 0.17$, p = 0.68, n = 192; HIS, $X^2 = 0.5$, p = 0.48, n = 180; UNC, $X^2 = 0.5$, p = 0.48, n = 144). Multiple comparisons against NAV (Pearson's Chi square test, df = 1), control responses: ALA, $X^2 = 0.01$, p = 0.90; TRP, $X^2 = 0.58$, p = 0.45; HIS, $X^2 = 4.5$, p = 0.03; UNC, $X^2 = 1.06$, p = 0.30. Multiple comparisons against NAV (Pearson's Chi square test, df = 1), PIN responses: ALA, $X^2 = 0.50$, p = 0.48; TRP, $X^2 = 0.25$,p = 0.62; HIS, $X^2 = 0.38$,p = 0.54; UNC, $X^2 = 0.07$, p = 0.80.
e. Odor responses of two individual neurons under control conditions (different colors) and during PIN (orange). Top: PIN-induced disinhibition was non-uniform across odors. Bottom: PIN-induced disinhibition was largely uniform. Numbers below traces show odor-specific change indices. SD_{inh} shows s.d. across the four change indices, a measure of the non-uniformity of inhibition. Vertical scale bars: 20% ΔF/F; horizontal scale bars: 10 s.
f. Non-uniformity of inhibition. Filled bars (orange; 'CP') show mean non-uniformity of inhibition, calculated by comparing control to PIN trials. Hollow black bars ('CC') show the same analysis comparing control trials to each other. Hollow orange bars ('PP') show the same analysis comparing PIN trials to each other. Comparison 'CC' vs 'CP' (paired *t* test, two-sided): NAV, $t = -31.78$, $p = 4x10^{-168}$, n = 1433; ALA, $t = -30.05$, $p = 1x10^{-152}$, n = 1363; TRP, $t = -9.37$, $p = 2x10^{-20}$, n = 1650; HIS, $t = -10.09$, $p = 3x10^{-23}$, n = 1740; UNC, $t = -22.53$, $p = 2x10^{-93}$, n = 1151. Comparison 'PP' vs 'CP' (paired *t* test, two-sided): NAV, $t = 35.78$, $p = 7x10^{-201}$; ALA, $t = 36.72$, $p = 1x10^{-205}$; TRP, $t = 42.99$, $p = 2x10^{-271}$; HIS, $t = 41.14$, $p = 6x10^{-259}$; UNC, $t = 28.72$, $p = 4x10^{-137}$. Only PIN-modulated, responding neurons were considered for this analysis (Online Methods). Number of animals as in Fig. 4d. Box plot: as in (**a**).

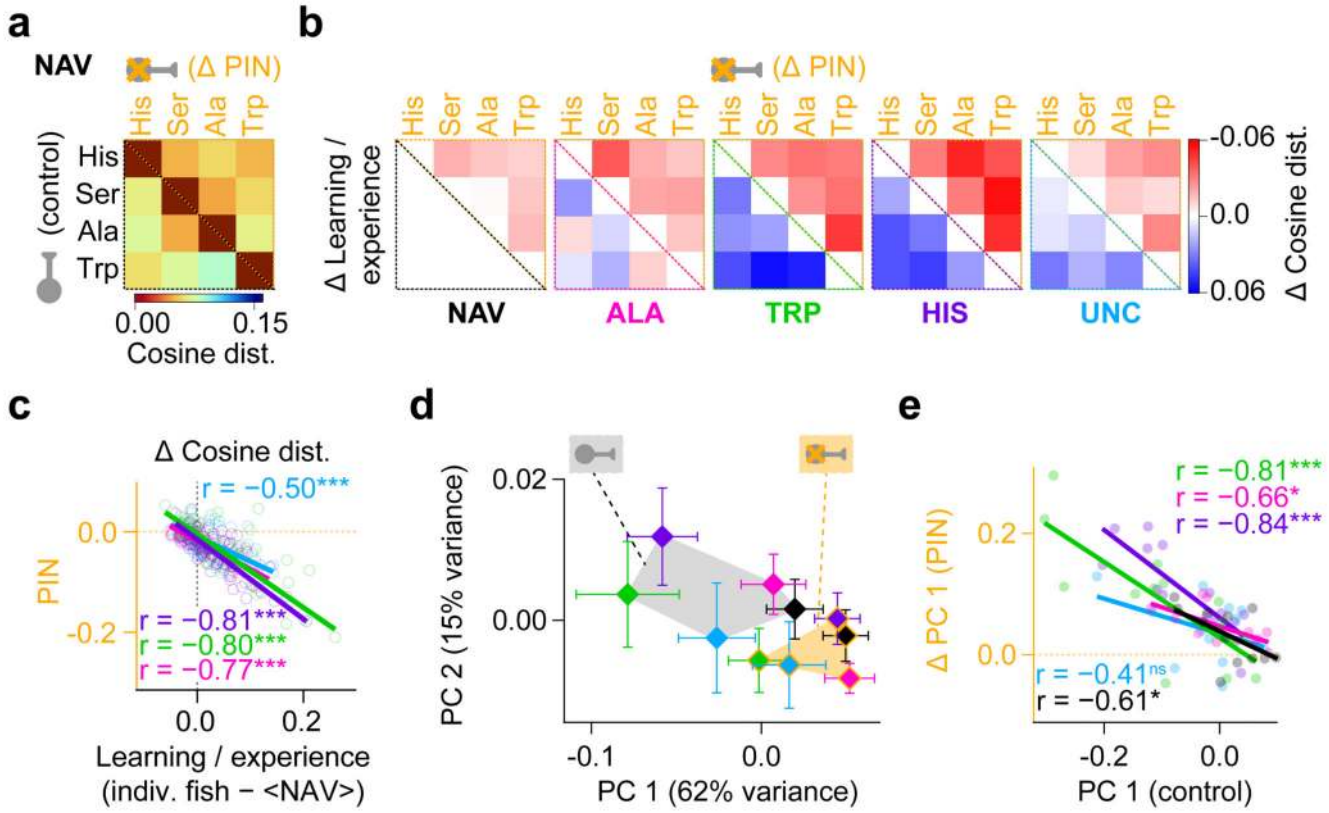

Fig. 8. Inhibition and reorganization of coding space

a. Cosine distances between odor-evoked activity patterns in NAV fish under control conditions (triangle below the diagonal; same as Fig. 1f) and during PIN (triangle above diagonal). Average cosine distance, control vs PIN, Wilcoxon signed rank test, two-sided: NAV, N = 13, T = 18, p = 0.06.

b. Effects of PIN and effects of experience on distances between odor-evoked activity patterns. Triangles above the diagonal show mean PIN-induced changes in pattern distance within the same fish ('Δ PIN', PIN – control). Triangles below the diagonal ('Δ Learning / experience') show mean difference in pattern distances relative to NAV fish under control conditions (ALA – NAV, TRP – NAV, HIS – NAV, UNC – NAV; identical to Fig. 4c). Average cosine distance, control vs PIN, Wilcoxon signed rank test, two-sided: ALA, N = 12, T = 0, p = 0.0004; TRP, N = 16, T = 9, p = 0.001; HIS, N = 15, T = 2, p = 0.0002; UNC, N = 12, T = 11, p = 0.03.

c. Correlation between effects of PIN-induced inhibition and effects of experience on pattern distances in individual fish. For each fish, the effect of PIN on pattern distances was measured by subtracting the distances under control conditions and during PIN (PIN – control; y-axis). The effect of experience on pattern distances was determined by subtracting the mean distance matrix of NAV fish from the distance matrix under control conditions (x-axis). Each plot symbol represents the observed distances changes for one odor pair in one fish. Significant negative correlations were observed in all groups (*t* test of null hypothesis of r = 0, two-sided, df = n-2; n is the number of distance values): ALA, r = –0.77, $t = -9.96$, p = $5\text{x}10^{-15}$, n = 72; TRP, r = –0.80, $t = -13.05$, p = $8\text{x}10^{-23}$, n = 96; HIS, r = –0.81, $t = -12.75$,

Europe PMC Funders Author Manuscripts

Europe PMC Funders Author Manuscripts

p = $1x10^{-21}$, n = 90; UNC, r = –0.50, t = –4.85, p = $7x10^{-6}$, n = 72. Kendall's rank correlation (test of null hypothesis of $\tau = 0$ using a normal approximation, two-sided): ALA, τ = –0.48, z = –5.95, p = $3x10^{-9}$; TRP, τ = –0.61, z = –8.82, p = $1x10^{-18}$; HIS, τ = –0.58, z = –8.14, p = $4x10^{-16}$; UNC, τ = –0.34, z = –4.26, p = $2x10^{-5}$.

d. PIN reduced distances between coding structures from different experimental groups. Diamonds represent group means (± s.e.m.) of coding structures projected onto the first two principal components. Polygons illustrate systematic differences between mean coding spaces of fish that were subjected to different experience. Gray polygon shows substantial differences between experimental groups under control conditions. Yellow polygon shows PIN-dependent shift of groups along the primary axes of coding space, compressing group differences and abolishing separability along the primary dimension (PC 1; Supplementary Fig. 6g). Number of animals as in Fig. 5b.

e. PIN-mediated change of PC 1 score as a function of PC 1 score under control conditions. The effect of PIN was significantly correlated to the control PC 1 score across all fish (Pearson correlation, df = N-2): r = –0.74 (t test of null hypothesis of r = 0, two-sided, t = –9.01, p = $4x10^{-13}$). Kendall's rank correlation: τ = –0.51 (test of null hypothesis of $\tau = 0$ using a normal approximation, two-sided, z = –6.20, p = $5x10^{-10}$). Significant negative correlations were also observed in all individual groups, except UNC (Pearson correlation): NAV, r = –0.61, t = –2.57, p = 0.03; ALA, r = –0.66, t = –2.80, p = 0.02; TRP, r = –0.81, t = –3.33, p = 0.0009; HIS, r = –0.84, t = –5.56, p = $9x10^{-5}$; UNC, r = –0.40, t = –1.42, p = 0.19. Kendall's rank correlation: NAV, τ = –0.33, z = –1.59, p = 0.11; ALA, τ = –0.39, z = –1.78, p = 0.07; TRP, τ = –0.62, z = –3.33, p = 0.0008; HIS, τ = –0.65, z = –3.41, p = 0.0006; UNC, τ = –0.15, z = –0.69, p = 0.49. Number of animals as in Fig. 4d. Similar observations were made along PC 2 (Supplementary Fig. 6h).